

2. Gutierrez G, Master SS, Singh SB: **Autophagy is a defense mechanism inhibiting BCG and Mycobacterium tuberculosis survival in infected macrophages.** *Cell* 2004, **119**:753-766.
3. Luo Yi, Szilvasi A, Chen X: **A novel method for monitoring Mycobacterium bovis BCG trafficking with recombinant BCG expressing green fluorescent protein.** *Clin Diagn Lab Immunol* 1996, **3**:761-768.
4. Shen Z, Wang Y, Ding GQ: **Study on enhancement of fibronectin-mediated bacillus Calmette-Guérin attachment to urinary bladder wall in rabbits.** *World J Urol* 2007, **25**:525-529.
5. Harboe M, Nagai N: **MPB70, a unique antigen of Mycobacterium bovis BCG.** *Am Rev Respir Dis* 1984, **129**:444-452.
6. Nagai S, Wiker HG, Harboe M: **Isolation and partial characterization of Major protein antigens in the culture fluid of Mycobacterium tuberculosis.** *Infect Immun* 1991, **59**:372-382.
7. Mastumoto S, Matsuo T, Ohara N: **Cloning and sequencing of a unique antigen MPT70 from Mycobacterium tuberculosis H37Rv and expression in BCG using E. coli-Mycobacteria Shuttle Vector.** *Scand J Immunol* 1995, **41**:281-287.
8. Decobert M, LaRue H, Harel F: **Maintenance bacillus Calmette-Guérin in high-risk nonmuscle-invasive bladder cancer. How much is enough?** *Cancer* 2008, **113**:710-716.
9. Kuroda K, Brown EJ, Telle WB: **Characterization of the internalization of bacillus Calmette-Guérin by human bladder tumor cells.** *J Clin Invest* 1993, **91**:69-76.
10. Ohara N, Kitaura H, Hotokezaka H: **Characterization of the gene encoding the MPB51, one of the major secreted protein antigens of Mycobacterium bovis BCG, and identification of the secreted protein closely related to the fibronectin binding 85 complex.** *Scand J Immunol* 1995, **41**:433-442.
11. Kuromatsu I, Matsuo K, Takamura S: **Induction of effective anti-tumor immune responses in a mouse bladder tumor model by using DNA of an  $\alpha$  antigen from mycobacteria.** *Cancer Gene Ther* 2001, **8**:483-490.
12. Mitropoulos DN: **Novel insights into the mechanism of action of intravesical immunomodulators.** *In vivo* 2005, **19**:611-612.
13. Sinn HW, Elzey BD, Jensen RJ: **The fibronectin attachment protein of bacillus Calmette-Guérin (BCG) mediates antitumor activity.** *Cancer Immunol Immunother* 2008, **57**:573-579.
14. Oh BR, Jeong DW: **Antitumor effects of bcg and cytokines against MBT-2 mouse bladder tumor cell.** *Bri J Urol* 1997, **80**(SUPPL 45):.
15. Becich MJ, Carroll S, Ratiff TL: **Internalization of bacillus calmette-guérin by bladder tumor cells.** *J Urol* 1991, **145**:1316-1324.
16. Bevers RFM, De Boer EC, Kurth H: **BCG internalization in human bladder cancer cell lines, especially with regard to cell surface-expressed fibronectin.** *Actual Urol* 2000, **31**:31-34.
17. Biswas D, Qureshi OS, Lee W-Y: **ATP-induced autophagy is associated with rapid killing of intracellular mycobacteria within human monocytes/macrophages.** *BMC Immuno* 2008, **9**:35.
18. DiPaola RS, Lattime EC: **Bacillus Calmette-Guérin mechanism of action: The role of immunity, apoptosis, necrosis and autophagy.** *J Urolo* 2007, **178**:1840-1841.
19. Chen N, Karantza-Vadsworth V: **Role and regulation of autophagy in cancer.** *Biochim Biophys Acta* 2009, **1973**:1516-1523.
20. Inbal B, Bialik S, Sabanay I: **DAP kinase and DRP-1 mediate membrane blebbing and the formation of autophagic vesicles during programmed cell death.** *J cell boil* 2002, **157**:455-468.
21. Matsumoto S, Yukitake H, Kanbara H: **Mycobacterium bovis Bacillus Calmette-Guérin induces protective immunity against infection by Plasmodium yoelii at blood-stage depending on shifting immunity toward Th1 type and inducing protective IgG2a after the parasite infection.** *Vaccine* 2001, **19**:779-787.
22. Luo Y, Yamada H, Evanoff DP: **Role of Th1-stimulating cytokines in bacillus Calmette-Guérin(BCG)-induced macrophage cytotoxicity against mouse bladder cancer MBT-2 cells.** *Clin Exp Immunol* 2006, **146**:181-188.
23. Hotokezaka H, Kitamura A, Mastumoto S: **Internalization of Mycobacterium bovis Bacillus Calmette-Guérin into Osteoblast-like MC3T3-EL cells and bone resorptive response of the cells against the infection.** *Scand J Immunol* 1998, **47**:453-458.
24. Wei MQ, Mengesha A, Good D: **Bacterial targeted tumour therapy-dawn of a new area.** *Cancer Lett* 2008, **259**:16-17.
25. Zbar B, Rapp HJ: **Immunotherapy of guinea pig cancer with BCG.** *Cancer* 1974, **34**:1532-1540.
26. Kitamura A, Tobita T, Fuzisawa A: **Evaluation on the cell-killing effects of the alpha-antigen by electroporation.** *Jpn J Cancer Res* 2001, **92**(Supp 555):.
27. Morales A: **Evolution of intravesical immunotherapy for bladder cancer: Mycobacterial cell wall preparation as a promising agent.** *Expert Opin Investig Drugs* 2008, **17**:1067-1073.
28. Kitamura A: **Bleomycin-mediated electrochemotherapy in mouse NR-S1 carcinoma.** *Cancer Chemother Pharmacol* 2003, **51**:359-362.
29. Ikeda N, Honda I, Yano I: **Bacillus Calmette-Guérin Tokyo172 substrain for superficial bladder cancer: Characterization and antitumor effect.** *J Urolo* 2005, **173**:1507-1512.

Publish with **BioMed Central** and every scientist can read your work free of charge

"BioMed Central will be the most significant development for disseminating the results of biomedical research in our lifetime."

Sir Paul Nurse, Cancer Research UK

Your research papers will be:

- available free of charge to the entire biomedical community
- peer reviewed and published immediately upon acceptance
- cited in PubMed and archived on PubMed Central
- yours — you keep the copyright

Submit your manuscript here:  
[http://www.biomedcentral.com/info/publishing\\_adv.asp](http://www.biomedcentral.com/info/publishing_adv.asp)



## Mycolyltransferase from *Mycobacterium leprae* Excludes Mycolate-containing Glycolipid Substrates

Hitomi Nakao<sup>1,2,\*</sup>, Isamu Matsunaga<sup>1,2,\*†</sup>, Daisuke Morita<sup>1,2</sup>, Takako Aboshi<sup>3</sup>, Toshiyuki Harada<sup>3</sup>, Yoshiaki Nakagawa<sup>3</sup>, Naoki Mori<sup>3</sup> and Masahiko Sugita<sup>1,2</sup>

<sup>1</sup>Laboratory of Cell Regulation, Institute for Virus Research, Kyoto University; <sup>2</sup>Laboratory of Cell Regulation and Molecular Network, Graduate School of Biostudies; and <sup>3</sup>Division of Applied Life Sciences, Graduate School of Agriculture, Kyoto University, Kyoto 606-8502, Japan

Received June 23, 2009; accepted July 3, 2009; published online July 23, 2009

Trehalose dimycolate (TDM) is a major surface-exposed mycolyl glycolipid that contributes to the hydrophobic cell wall architecture of mycobacteria. Nevertheless, because of its potent adjuvant functions, pathogenic mycobacteria appear to have evolved an evasive maneuver to down-regulate TDM expression within the host. We have shown previously that *Mycobacterium tuberculosis* (M.tb) and *Mycobacterium avium* (M.av), replace TDM with glucose monomycolate (GMM) by borrowing host-derived glucose as an alternative substrate for the FbpA mycolyltransferase. *Mycobacterium leprae* (M.le), the causative microorganism of human leprosy, is also known to down-regulate TDM expression in infected tissues, but the function of its mycolyltransferases has been poorly analysed. We found that, unlike M.tb and M.av FbpA enzymes, M.av FbpA was unexpectedly inefficient in transferring  $\alpha$ -branched mycolates, resulting in impaired production of both TDM and GMM. Molecular modelling and mutational analysis indicated that a bulky side chain of leucine at position 130 of M.le FbpA obstructed the intramolecular tunnel that was proposed to accommodate the  $\alpha$ -branch portion of the substrates. Notably, even after a highly reductive evolution, M.le FbpA remained functional in terms of transferring unbranched acyl chains, suggesting a role that is distinct from that as a mycolyltransferase.

**Key words:** glycolipid, glucose monomycolate, *Mycobacterium leprae*, mycolyltransferase, trehalose dimycolate.

Abbreviations: Fbp, fibronectin-binding protein; GMM, glucose monomycolate; M.av, *Mycobacterium avium*; M.le, *Mycobacterium leprae*; M.tb, *Mycobacterium tuberculosis*; TDM, trehalose dimycolate; TMM, trehalose monomycolate.

Mycobacteria are unique in their highly lipid-rich cell wall that is critical not simply for their acid-fast properties but also for their survival and replication. The cell wall contains mycolic acids, a family of  $\alpha$ -branched,  $\beta$ -hydroxy long-chain fatty acids, which are densely aligned in covalent association with the underlying arabinogalactan sugar layer or exist as free molecules complexed to either trehalose or glucose. The arabinogalactan-bound mycolic acids are proposed to extend outwards and interact closely with carbon chains of the surface-exposed glycolipids, thereby forming the hydrophobic cell wall architecture that is essential for long-term survival of pathogenic mycobacteria within host cells (1).

Trehalose-6,6'-dimycolate (TDM) comprises a major surface-exposed mycolyl glycolipid that can be readily synthesized when mycobacteria are cultured in artificial

media, and therefore, its biological activities as well as its relevance to pathogenesis have been studied extensively over the past two decades. A single dose of TDM can induce granuloma formation *in vivo* in animal tissues, and its outstanding ability to stimulate host innate immune cells, such as macrophages and dendritic cells, has been fully documented (2). Further, we recently reported TDM-elicited eosinophilic responses in mycobacteria-infected guinea pigs (3). All of these immunostimulatory or adjuvant functions mediated by TDM could potentially jeopardize the microbes by allowing the host to efficiently monitor and control infection. The generally accepted picture of the cell wall structure of mycobacteria, highlighting abundant TDM expression at the outermost layer, has been drawn, based primarily on biochemical analysis of the microbes cultivated in artificial media, but adaptive changes that minimize TDM functions may occur after pathogenic mycobacteria infect into the host.

Indeed, we have recently shown that a switch of glycolipid biosynthesis from TDM to another surface-exposed mycolyl glycolipid, glucose-6-monomycolate (GMM), occurs in *Mycobacterium tuberculosis* (M.tb) and *Mycobacterium avium* (M.av) upon exposure to host-derived glucose (4). Previous studies have

\*These two authors contributed equally to this work.

†To whom correspondence should be addressed. Tel: +81-75-751-4047, Fax: +81-75-752-3232.

E-mail: i\_matsun@virus.kyoto-u.ac.jp

Correspondence may also be addressed to Masahiko Sugita.

Tel: +81-75-751-4028, Fax: +81-75-752-3232,

E-mail: msugita@virus.kyoto-u.ac.jp

established that the final step of TDM biosynthesis is catalysed by the mycolyltransferase activity of the fibronectin-binding protein (Fbp), using its biosynthetic precursor, trehalose-6-monomycolate (TMM) as a substrate (5). However, at the physiological concentration of glucose present in mammalian hosts, TDM down-regulation and concomitant GMM up-regulation occur within hours as a result of competitive acceptor substrate selection of TMM and glucose by the Fbp enzyme (4). Given that GMM is much less potent than TDM in stimulating innate immune cells, the swift switch from TDM to GMM biosynthesis by utilizing the pre-existing Fbp enzyme and the host-derived glucose could function as an efficient evasive maneuver for pathogenic mycobacteria (4).

Leprosy is an ancient disease caused by *Mycobacterium leprae* (M.le) infection, but remains an important health problem worldwide. Unlike M.tb and M.av, M.le is not cultivable in artificial media, and therefore, its lipid chemistry and biology have not been studied so extensively as for the other pathogenic mycobacteria species. Previous studies have suggested that only a trace amount of TDM is produced by M.le grown in infected tissues while production of its biosynthetic precursor, TMM, is readily detectable (6). Nevertheless, the M.tb and the M.le genomes share all the four Fbp genes (*fbpA*, *fbpB*, *fbpC* and *fbpD*), and the deduced amino acid sequences indicate that products of M.le *fbpA*, *fbpB* and *fbpC*, designated FbpA, FbpB and FbpC, respectively, contain a catalytic triad that is essential for the mycolyltransferase activity, as found in other serine esterases (7). Therefore, it was initially hypothesized that M.le should have evolved an efficient strategy for TDM down-regulation that might be similar to maneuvers employed by M.tb and M.av. Surprisingly, however, we provide evidence that the M.le-derived FbpA protein excludes mycolate-containing glycolipid substrates, resulting in profound down-regulation of both TDM and GMM. This 'intrinsic' mechanism of TDM down-regulation has not been observed for other pathogenic mycobacteria species tested so far, and may uniquely support survival of M.le within the host.

#### MATERIALS AND METHODS

**Chemical Reagents and Bacteria**—Chemical reagents were purchased from Nacalai Tesque (Kyoto, Japan) unless otherwise indicated. *Mycobacterium avium* ATCC 35767 (serovar 4) was obtained from American Type Culture Collection (Manassas, VA, USA). The bacteria were grown in Middlebrook 7H9 media (BD, Franklin Lakes, NJ, USA) supplemented with the albumin-dextrose-catalase enrichment (BD) and 0.05% Tween 80. *Corynebacterium matruchotii* JCM 9386 was obtained from Japan Collection of Microorganisms (Tsukuba, Japan), and maintained on a plate of brain-heart-infusion agar media (BD). For isolation of TMM from *C. matruchotii*, the bacteria were grown in brain-heart-infusion liquid media containing 5% trehalose.

**Preparation of Recombinant Enzymes**—The recombinant M.av FbpA was prepared as described previously (4). The gene that encoded the mature M.le FbpA protein

lacking the signal sequence was amplified by PCR, using genomic DNA of the M.le Thai-53 strain (8) as a template and a specific primer set as follows: 5'-ggaattcca tatgttctccggccgggattgcc-3' (sense primer) and 5'-cccaagct tagcaccgggtagcccta-3' (antisense primer). The amplified PCR product was digested with NdeI and HindIII, and ligated to a NdeI-HindIII-digested pET-21c plasmid vector (Merck Japan, Tokyo, Japan). The nucleotide sequence of the cloned M.le *fbpA* was identical to that reported elsewhere (<http://genolist.pasteur.fr/Leproma/>). To optimize the codon usage for efficient expression in *Escherichia coli*, PCR was carried out with the cloned M.le *fbpA* gene as a template and a primer set as follows: 5'-cgcatatgttctctcgtccgggtctgccggttgagtacctgcaa-3' and 5'-gccccgggtagcaccagggtactgctgcagggtccggtttcatg-3' (sense and antisense primers, respectively, in which mutated nucleotides are underlined). The PCR product was digested with NdeI and SmaI, and exchanged for the corresponding fragment of the cloned M.le *fbpA* gene in pET-21c.

Site-directed mutagenesis was performed by PCR with the PrimeStar HS DNA polymerase (Takara Co. Ltd, Tokyo, Japan), using the codon-modified plasmids as a template. The primer sets used were as follows: 5'-cgg ttctcggcctgacgctggcgatctaccacc-3' and 5'-ggcgaagaaccg gccatcgaagaccgaccgccc-3' (for M.le *fbpA*); 5'-cggcctgtcgg cgctgatctggcgcctaccac-3' and 5'-cgcagaggccgcatcgac aggcgacgacacc-3' (for M.av *fbpA*), in which mutated nucleotides are underlined. The cycling conditions for PCR amplification were as follows: 95°C, 1 min, followed by 10 cycles of 95°C, 15 s and 72°C, 10 min, and a final extension step of 72°C, 10 min. The amplified PCR products were digested with DpnI, and used for transformation of *E. coli*. Introduction of the mutation was confirmed by DNA sequencing.

*Escherichia coli* BL21 (DE3) was transformed with each of the plasmids, and the His-tagged recombinant FbpA proteins were obtained as described (4) with slight modifications. The protein expression was induced with 0.1 mM IPTG at 25°C for 20 h. The cells were then harvested and disrupted by sonication in ice-cold 20 mM Tris-HCl (pH 7.9) buffer containing 0.5 M NaCl and 60 mM imidazole (sonication buffer). The sonicates were centrifuged at 6,000g for 30 min at 4°C to remove insoluble materials, and the supernatants were applied onto a Ni-resin column equilibrated with the sonication buffer. After washing the column with the sonication buffer, the recombinant proteins were eluted with the 20 mM Tris-HCl (pH 7.9) containing 0.5 M NaCl and 0.5 M imidazole. The eluates were concentrated and dialyzed overnight at 4°C against 50 mM sodium phosphate buffer (pH 7.5) containing 10% glycerol at 4°C. Purity and quantity of the enzymes were assessed by SDS-PAGE and Coomassie staining.

**Preparation of Substrates**—The M.av serovar 4-derived long-chain TMM was purified as described (4). For purification of the *C. matruchotii*-derived short-chain TMM, the cultured cells were harvested, and lipids were extracted with chloroform/methanol (C/M, 1:1, v/v), followed by fractionation by TLC with a solvent system of C/M/water (65:25:4, v/v/v). The TMM fraction was then extracted with C/M (1:1, v/v) from the silica gels.

The identity of the purified TMM preparations was confirmed by mass spectrometry.

Trehalose-6-monolaurate (TML) was synthesized by modification of a method of Raku *et al.* (9). The reaction mixture (dimethylformamide/water, 97:3, v/v) containing 160 mM  $\alpha$ -trehalose (Wako Pure Chemicals Co. Ltd., Osaka, Japan), 450 mM vinyl laurate (Tokyo Chemical Industry Co., Ltd, Tokyo, Japan) and 31 mg/ml Biopraxe OP (Nagase Chemtex Co. Ltd, Osaka, Japan) was incubated at 35°C for 7 days, and then extracted with *n*-hexane to remove unreacted vinyl laurate. The dimethylformamide phase was applied onto a C18 reverse-phase column (Presep C18 ODS, Wako Pure Chemicals) that was equilibrated with water. Subsequently, the column was washed with water, and the TML-containing fraction was eluted with acetonitrile/water (50:50, v/v). After evaporation, the fraction was dissolved in methanol and applied onto a silica gel G TLC plate (Analtech, Newark, NJ, USA). The plate was developed with a solvent system of C/M/acetone/acetic acid (50:30:20:1, v/v/v/v), and TML was extracted from the gel. Its identity was confirmed by mass spectrometry and <sup>1</sup>H NMR.

**Enzyme Assays**—FbpA enzyme assays were performed as described (4) with slight modifications. Each of the lipidic substrates (63  $\mu$ M long-chain TMM, 130  $\mu$ M short-chain TMM and 1.9 mM TML) was prepared in 20 mM sodium phosphate buffer (pH 7.5) (reaction buffer) unless otherwise indicated. In experiments monitoring GMM production, the reaction mixtures also contained 4% D-glucose (w/v). The reaction was started by the addition of either *M.le*-derived or *M.av*-derived FbpA enzymes (1.5 nmol for long-chain TMM, 160 pmol for short-chain TMM, and 7.8 pmol for TML) with a total volume of 200  $\mu$ l per tube, and after 20 min of incubation at 37°C, the reaction was stopped by the addition of 3 ml of C/M (2:1) and 0.3 ml of distilled water as well as *n*-tetradecanol (20  $\mu$ g per sample) that served as an indicator for extraction efficiency. The lipids were extracted by the method of Kremer *et al.* (10) and analysed by silica gel TLC with a solvent of either C/M/acetone/acetic acid (90:10:10:1) (for detection of long-chain mycolyl glycolipids) or C/M/acetone/acetic acid (80:15:10:1) (for detection of lauryl trehalose and short-chain mycolyl glycolipids). The lipids on the TLC plates were visualized by spraying 50% sulphuric acid and baking. The amounts of each compound were calculated, based on the intensity of spots of serially diluted *n*-tetradecanol. The molecular identity of the products was confirmed by mass spectrometry, using an electrospray-ion trap-time of flight mass spectrometer (Shimadzu LCMS-IT-TOF, Shimadzu Co. Ltd, Kyoto, Japan) as described (11).

**Kinetic Analysis of Enzyme Reactions**—Enzyme assays were carried out with wild-type and mutant FbpA enzymes, using four different concentrations of the *C. matruchoii*-derived short-chain TMM as a substrate. The lipids were extracted and separated on TLC plates, followed by densitometrical determination of the amount of the products, using serially diluted *n*-tetradecanol as a reference. Data were collected from three independent experiments, and kinetic analysis was performed by Hanes-Woolf plotting.

**Molecular Modelling of the FbpA S130L Mutant**—Molecular modelling of the *M.tb*-derived FbpA S130L mutant protein was performed, using the homology modelling software PDFAMS (Protein Discovery Full Automatic Modeling System; In-Silico Sciences, Inc., Tokyo, Japan) as described (12, 13). Briefly, the primary sequence and the molecular model of the *M.tb* FbpA protein were obtained from the Protein Data Bank (1SFR). The serine residue at position 130 was mutated into leucine, and the obtained 3D structure was optimized by the simulated annealing method. Subsequently, the molecular model was subjected to energy minimization, using the SYBYL software (version 7.3; Tripos Inc., St Louis, MO, USA). The surface of the channel that was proposed to accommodate the  $\alpha$ -branch portion of the substrates was depicted by utilizing the MOLCAD module of SYBYL.

## RESULTS

***M.le* FbpA Exhibits Reduced Mycolyltransferase Activity**—Recombinant FbpA enzymes derived from *M.le* and *M.av* were obtained and tested for their mycolyltransferase activity in an *in vitro* enzyme assay, using mycobacteria-derived natural TMM as a substrate. As we have shown previously (4), an efficient transfer of the mycolyl acyl group from one TMM substrate (donor) to the other TMM substrate (acceptor) occurred in the presence of the *M.av* FbpA protein, evidenced by generation of the reaction product, TDM (Fig. 1, lane 1).

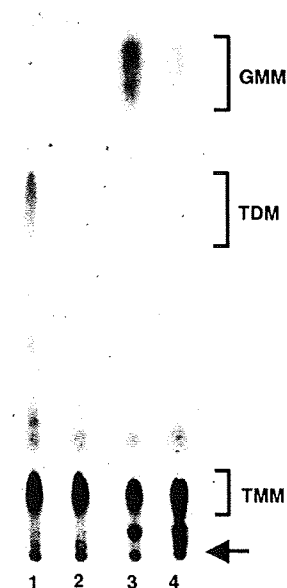


Fig. 1. Reduced mycolyltransferase activity of *M.le* FbpA. Enzymatic reactions with the long-chain TMM as a substrate were performed at 37°C for 20 min at conditions indicated below, and the lipids were extracted from the reaction mixtures, followed by analysis on a TLC plate. Lane 1, *M.av* FbpA and TMM; lane 2, *M.le* FbpA and TMM; lane 3, *M.av* FbpA, TMM and glucose; lane 4, *M.le* FbpA, TMM and glucose. The TLC origin is indicated with an arrow.

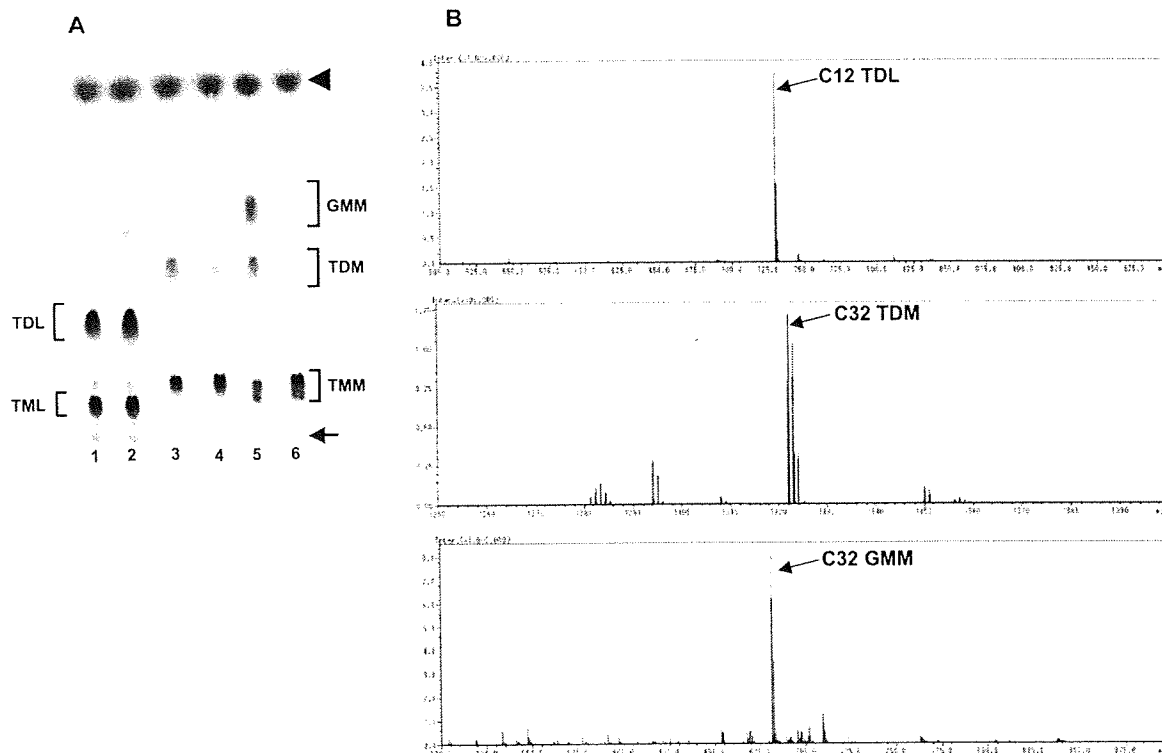


Fig. 2. Efficient utilization of unbranched, but not  $\alpha$ -branched, substrates by *M.le* FbpA. (A) Enzymatic reactions were performed as in Fig. 1, using either TML or the short-chain TMM as a substrate. Lane 1, *M.av* FbpA and TML; lane 2, *M.le* FbpA and TML; lane 3, *M.av* FbpA and TMM; lane 4, *M.le* FbpA and TMM; lane 5, *M.av* FbpA, TMM and glucose; lane 6, *M.le* FbpA, TMM and glucose. The position of the extraction efficiency indicator, *n*-tetradecanol, is indicated with an arrowhead. Note that equivalent amounts of *n*-tetradecanol

were visualized throughout the lanes. (B) The reaction products, TDL (top panel), *C. matruchoyii* TDM (middle panel) and GMM (bottom panel), were extracted from the TLC plates and analysed by mass spectrometry. The major ions of  $m/z$  729.4 (top panel),  $m/z$  1322.0 (middle panel) and  $m/z$  681.5 (bottom panel) were indicated with arrows that represent sodium adducts of  $C_{12}$  TDM, TDM with two molecules of  $C_{32}$  mycolate, and  $C_{32}$  mycolate-containing GMM, respectively.

In sharp contrast, only a tiny amount of TDM was detected when an equivalent amount of the *M.le* FbpA protein was used (lane 2). The mycolyltransferase activity of the *M.av* and *M.le* FbpA proteins was also assessed in parallel, using glucose as an alternative acceptor substrate. Similar to TDM, much more efficient generation of the reaction product, GMM, was observed for *M.av* FbpA (lane 3), and only a trace of GMM was produced by *M.le* FbpA (lane 4). Therefore, these results detected apparently reduced mycolyltransferase activity for *M.le* FbpA.

*M.le* FbpA Retains the Ability to Transfer Unbranched, but not  $\alpha$ -branched, Fatty Acids—The mycobacteria-derived TMM molecules used as a substrate for the enzyme reactions above were those containing  $\alpha$ -branched, long-chain (mainly  $C_{85}$ ) fatty acids. To gain insight into the molecular basis for the decreased mycolyltransferase activity exhibited by *M.le* FbpA, similar *in vitro* enzyme reaction experiments were performed, using two monoacyl trehalose compounds as model substrates; namely, synthesized TML with a  $C_{12}$  unbranched acyl chain, and *C. matruchoyii*-derived TMM with

$\alpha$ -branched, short-chain (mainly  $C_{32}$ ) fatty acids. We found that both *M.av* and *M.le* FbpA proteins were capable of transferring the  $C_{12}$  unbranched acyl chain from the donor TML molecule to the acceptor TML molecule efficiently, resulting in generation of a comparable amount of trehalose-6,6'-dilaurate (TDL) by both enzymes (Fig. 2A, lanes 1 and 2). The molecular identity of the product as TDL was confirmed by mass spectrometry, in which the mass numbers of given ions were matched with those for sodium adducts of  $C_{12}$  TDL (Fig. 2B, top panel). On the other hand, the *C. matruchoyii*-derived  $\alpha$ -branched, short-chain TMM was not utilized efficiently as a donor substrate for *M.le* FbpA, evidenced by reduced TDM and GMM production as compared with *M.av* FbpA (Fig. 2A, lane 3 versus lane 4 for TDM production, and lane 5 versus lane 6 for GMM production). The molecular identity of the products as TDM and GMM was confirmed by mass spectrometry (Fig. 2B, middle and bottom panels, respectively). From these observations, we hypothesized that, unlike monoacyl trehalose compounds with an unbranched fatty acid, those containing the fatty acyl branching of mycolic acids could

not gain easy access to the donor substrate-binding site of the *M.le* FbpA protein.

**Leucine at Position 130 of *M.le* FbpA Limits Access of Mycolate-containing Glycolipid Substrates to their Binding Site**—Crystallographic studies of *M.tb*-derived mycolyltransferases detected a tunnel extending through the core of the protein that could accommodate the  $\alpha$ -branch portion of mycolates while their meromycolate chain fitted in a long cleft formed on the surface of the enzyme (14–16). The fact that even the  $\alpha$ -branch of the short-chain TMM could not be efficiently utilized by the *M.le* FbpA enzyme might indicate a failure of the  $\alpha$ -branch to penetrate deeply into the tunnel due to blockade at or near its opening. We therefore looked closely at the  $\alpha 4$  helix (Fig. 3A, boxed area) that contributed to the formation of the tunnel in the proximity of the position 126 serine residue (indicated with an asterisk) of the catalytic triad. Alignment of the amino acid sequences of *M.le*-, *M.av*- and *M.tb*-derived FbpA proteins shows that the  $\alpha 4$  helix sequence is highly conserved, but the position 130 serine residue found in both

*M.av* and *M.tb* is replaced by leucine in *M.le* (Fig. 3, indicated with an arrowhead).

In the crystal structure of the *M.tb* FbpA protein reported previously, the side chain of the position 130 serine residue (Ser130) protrudes into the lumen of the tunnel (demarcated with dotted lines), generating a kinky channel, but there is still a plenty of open space that allows smooth accommodation of the  $\alpha$ -branch portion of the substrates (Fig. 3B, left panel). On the other hand, molecular modeling after serine-to-leucine mutation was introduced at position 130 revealed that the bulky side chain of the leucine residue protruded further, resulting in total obstruction of the tunnel (Fig. 3B, right panel). Thus, we suspected that the impaired utilization of  $\alpha$ -branched fatty acid-containing substrates by *M.le* FbpA might be accounted for by the presence of the leucine residue at position 130.

To test this possibility directly, recombinant *M.le*- and *M.av*-derived FbpA proteins with a single amino acid mutation at position 130 were generated and assessed for their acyl-chain transfer activity. The mutant *M.av* FbpA protein in which the serine residue was replaced with leucine (*M.av* FbpA S130L) exhibited a reduced mycolyltransferase activity (Fig. 4A, lane 4) as compared with the wild-type *M.av* FbpA protein (lane 3) while maintaining the ability to transfer the C<sub>12</sub> unbranched acyl chain (lanes 1 and 2). In sharp contrast, the mutant *M.le* FbpA protein in which the leucine residue was replaced with serine (*M.le* FbpA L130S) exhibited an enhanced mycolyltransferase activity (Fig. 4B, lane 4) as compared with the wild-type *M.le* FbpA

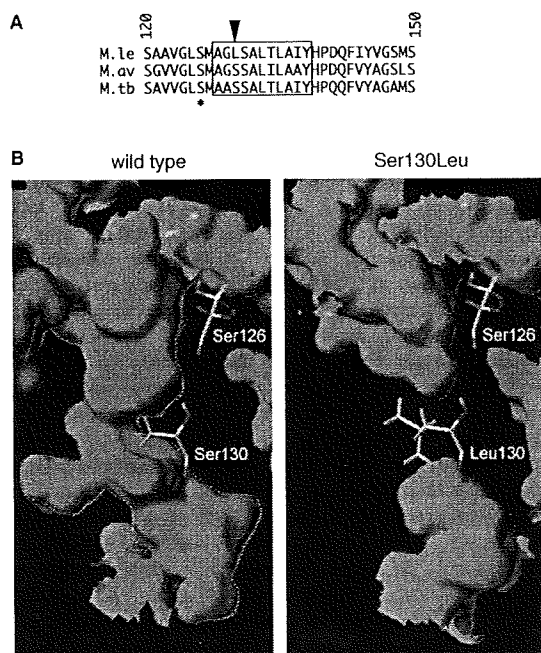


**Fig. 3. A critical amino acid residue at position 130 of FbpA proteins that regulates interaction with  $\alpha$ -branched substrates.** (A) Partial amino acid sequences of *M.le*-, *M.av*- and *M.tb*-derived FbpA proteins are aligned. Residues from position 120 to position 150 are shown, and the position 130 is indicated with an arrowhead. The boxed area indicates amino acid sequences of the  $\alpha 4$  helix. The serine residue of the catalytic triad located at position 126 is indicated with an asterisk. (B) Structure of the *M.tb* wild type FbpA (left panel) and molecular modeling of its Ser130Leu mutant (right panel) are shown. The surface of open space is depicted, and the intramolecular channel that accommodates the  $\alpha$ -branch portion of the substrates is demarcated with dotted lines. Note that the tunnel totally collapsed after the introduction of the mutation.

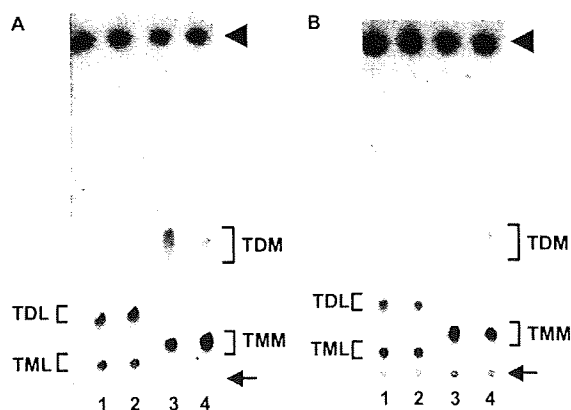


**Fig. 4. Effects of amino acid substitution at position 130 of FbpA proteins on mycolyltransferase activity.** (A) Enzymatic reactions were performed with either the wild-type *M.av* FbpA or its mutant (*M.av* FbpA S130L) as in Fig. 1 except for the use of TML at 0.3 mM. Lane 1, wild-type *M.av* FbpA and TML; lane 2, *M.av* FbpA S130L and TML; lane 3, wild-type *M.av* FbpA and short-chain TMM; lane 4, *M.av* FbpA S130L and short-chain TMM. (B) Similar enzymatic reactions were performed with either the wild-type *M.le* FbpA or its mutant (*M.le* FbpA L130S). Lane 1, wild-type *M.le* FbpA and TML; lane 2, *M.le* FbpA L130S and TML; lane 3, wild-type *M.le* FbpA and short-chain TMM; lane 4, *M.le* FbpA L130S and short-chain TMM. The TLC origin and the position of *n*-tetradecanol are indicated with arrows and arrowheads, respectively.

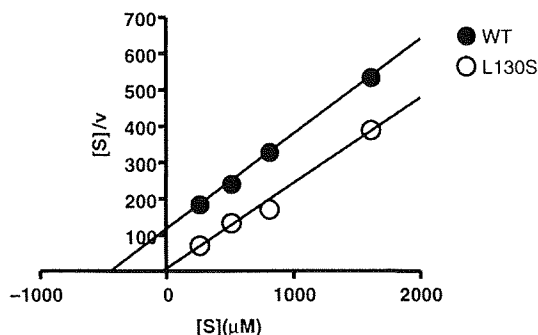


Fig. 5. Distinct enzyme kinetics for *M.le* wild-type and mutant FbpA proteins. Enzyme assays were performed with either wild-type or mutant FbpA proteins, using different concentrations of the short-chain TMM as a substrate. The lipids were extracted, and the amount of the product was densitometrically determined on TLC plates. Hanes-Woolf plots are shown for the wild-type (closed circles) and the mutant (open circles) FbpA enzymes.

protein (lane 3), while the ability to transfer the unbranched acyl chain was unchanged (lanes 1 and 2).

To quantitatively assess the enzyme activity of the *M.le* FbpA wild-type and mutant proteins, enzyme assays were carried out in the presence of varying amounts of the short-chain TMM substrate, and the amount of the product, TDM, generated at each concentration was determined, followed by kinetic analysis of the reactions using Hanes-Woolf plotting. As shown in Fig. 5, separate, but almost parallel, linearity was obtained for the wild-type and mutant enzymes, indicating a sharp decrease in the apparent  $K_m$  value after the amino acid substitution while the  $V_{max}$  values remained almost unaffected. The calculated  $K_m$  values were  $459 \mu\text{M}$  for the wild-type and  $43 \mu\text{M}$  for the mutant, and the  $V_{max}$  values were  $3.83 \text{ nmol/min/nmol enzyme}$  for the wild-type and  $4.27 \text{ nmol/min/nmol enzyme}$  for the mutant, underscoring an increased affinity of the TMM substrate to the mutant enzyme. Therefore, the amino acid substitution experiments detected a critical role for the leucine residue at position 130 in excluding  $\alpha$ -branched mycolates, which could account for the reduced mycolyltransferase activity of the *M.le* FbpA enzyme.

#### DISCUSSION

TDM is produced abundantly by virtually all cultivable mycobacterial pathogens, and its relevance to pathogenesis has been proposed (1, 2). Nevertheless, given its potent adjuvant effects on a wide variety of host immune cells, it would be reasonable to speculate that, upon infection into the host, pathogenic mycobacteria may down-regulate the TDM expression to allow for their escape from the host immune system. In this respect, the mycolyltransferase-mediated switch of glycolipid biosynthesis from TDM to GMM by borrowing host-derived glucose could function as an exquisite maneuver that pathogenic mycobacteria, such as *M.tb* and *M.av*, are able to employ (4). The cell wall lipid components

of *M.le* remain to be fully characterized due to the highly limited sources of the microbe, but it has been suggested that the expression of TDM could be far below the level that would be expected for other mycobacteria (6), implicating a highly efficient mechanism for TDM down-regulation. Therefore, it is important to determine how TDM biosynthesis is regulated in *M.le* in order to understand the unique immunopathological features of leprosy.

The function of *M.le*-derived mycolyltransferases has not been specifically addressed previously. By utilizing recombinant proteins and an array of substrates in *in vitro* enzyme assays, the present study has disclosed for the first time unexpected features of the *M.le*-derived FbpA enzyme that are unique to *M.le*, but not to other pathogenic mycobacteria. Unlike the *M.av* FbpA protein capable of catalysing TDM synthesis from its precursor, TMM, the *M.le* enzyme was inefficient as a mycolyltransferase to generate TDM while maintaining its catalytic activity to transfer an unbranched acyl chain (Figs 1 and 2). Further, the site-directed mutagenesis studies, identifying the amino acid residue at position 130 as a key determinant for the accessibility of the  $\alpha$ -branch portion of mycolates, have provided a molecular basis for the reduced mycolyltransferase activity of the *M.le* FbpA enzyme (Figs 4 and 5). Thus, these observations underscore 'intrinsic' defects of TDM production in *M.le*, which contrasted sharply with the 'extrinsic' pathway for TDM down-regulation in other pathogenic mycobacteria, borrowing host-derived glucose as an alternative substrate for their functional mycolyltransferases (4). Whereas the extrinsic pathway involves concomitant up-regulated expression of GMM, a specific target for host CD1b-restricted cytotoxic T cells that can detect and lyse mycobacteria-infected cells (17, 18), the simultaneous down-regulation of TDM and GMM expression achieved by the intrinsic mechanism would minimize activation of both innate and acquired phases of host immunity, providing better chances for the microbe to survive in the host. Given that *M.le* is an obligate intracellular parasite that can survive only within the host cells, it might have been critically important for the bacteria to evolve highly efficient maneuvers for adaptation to host environments by even reducing the genuine function of mycolyltransferases. Transcription of *fbpA*, *fbpB* and *fbpC* genes could be detected during *M.le* growth (19). Nevertheless, its TDM expression is highly suppressed (6), implicating that the other mycolyltransferases, FbpB and FbpC, also fail to generate TDM. Unlike *M.le* FbpA that contains a unique amino acid at position 130, the corresponding amino acid residue in FbpB and FbpC is shared between *M.le* and *M.tb*. This suggests that distinct, but yet undetermined, mechanisms should have been evolved for *M.le* FbpB and FbpC that support TDM down-regulation.

As mentioned earlier, detailed lipid biochemical analysis of *M.le* has been hampered due to the limited sources of the bacteria. Nevertheless, the sequence of the recently decoded *M.le* genome (7) and its comparison with that of its close relative *M.tb* genome often provide a valuable clue that helps us to understand the yet undefined biology of *M.le*. The *M.le* genome is much smaller in size with more pseudogenes, resulting in

significantly reduced numbers of open reading frames that potentially encode functional proteins. It is noteworthy that, even after such a highly reductive evolution, the *M.le* genome still contains apparently functional *fbp* genes. Surprisingly, while specifically reducing the mycolyltransferase activity by blockade of the tunnel that accommodates the  $\alpha$ -branch of mycolates, the *M.le* FbpA protein still preserves the molecular structure for interaction with the unbranched glycolipid substrates and the catalytic activity to transfer the unbranched acyl chain (Fig. 2). This suggests that the protein integrity of the *M.le* FbpA has been maintained during the reductive evolution and that it might play a role in the lifecycle of *M.le*, which is distinct from that as a mycolyltransferase. The present study, detecting differential mycolyltransferase activity in *M.le* and other pathogenic mycobacteria, provides a clue to the still mysterious biology of the first human pathogenic bacterium to be identified.

## ACKNOWLEDGEMENTS

We thank Dr Shinji Maeda (Research Institute of Tuberculosis) for the gift of *M.le*-derived genomic DNA.

## FUNDING

Grants from the Ministry of Education, Culture, Sports, Science and Technology (Grant-in-Aid for Scientific Research on Priority Areas) (to M.S.); from the Japan Society for the Promotion of Science (Grant-in-Aid for Scientific Research (B) (to M.S.) and (C) (to I.M.)); from the Ministry of Health, Labour, and Welfare (Research on Emerging and Re-emerging Infectious Diseases) (to M.S.); the Shimizu Foundation Research Grant for 2007 (to I.M.).

## CONFLICT OF INTEREST

None declared.

## REFERENCES

- Brennan, P.J. (2003) Structure, function, and biogenesis of the cell wall of *Mycobacterium tuberculosis*. *Tuberculosis* **83**, 91–97
- Ryll, R., Kumazawa, Y., and Yano, I. (2001) Immunological properties of trehalose dimycolate (cord factor) and other mycolic acid-containing glycolipids—a review. *Microbiol. Immunol.* **45**, 801–811
- Otsuka, A., Matsunaga, I., Komori, T., Tomita, K., Toda, Y., Manabe, T., Miyachi, Y., and Sugita, M. (2008) Trehalose dimycolate elicits eosinophilic skin hypersensitivity in mycobacteria-infected guinea pigs. *J. Immunol.* **181**, 8528–8533
- Matsunaga, I., Naka, T., Talekar, R.S., McConnell, M.J., Katoh, K., Nakao, H., Otsuka, A., Behar, S.M., Yano, I., Moody, D.B., and Sugita, M. (2008) Mycolyltransferase-mediated glycolipid exchange in Mycobacteria. *J. Biol. Chem.* **283**, 28835–28841
- Belisle, J.T., Vissa, V.D., Sievert, T., Takayama, K., Brennan, P.J., and Besra, G.S. (1997) Role of the major antigen of *Mycobacterium tuberculosis* in cell wall biogenesis. *Science* **276**, 1420–1422
- Dhariwal, K.R., Yang, Y.M., Fales, H.M., and Goren, M.B. (1987) Detection of trehalose monomycolate in *Mycobacterium leprae* grown in armadillo tissues. *J. Gen. Microbiol.* **133**, 201–209
- Cole, S.T., Eiglmeier, K., Parkhill, J., James, K.D., Thomson, N.R., Wheeler, P.R., Honore, N., Garnier, T., Churcher, C., Harris, D., Mungall, K., Basham, D., Brown, D., Chillingworth, T., Connor, R., Davies, R.M., Devlin, K., Duthoy, S., Feltwell, T., Fraser, A., Hamlin, N., Holroyd, S., Hornsby, T., Jagels, K., Lacroix, C., Maclean, J., Moule, S., Murphy, L., Oliver, K., Quail, M.A., Rajandream, M.A., Rutherford, K.M., Rutter, S., Seeger, K., Simon, S., Simmonds, M., Skelton, J., Squares, R., Squares, S., Stevens, K., Taylor, K., Whitehead, S., Woodward, J.R., and Barrell, B.G. (2001) Massive gene decay in the leprosy bacillus. *Nature* **409**, 1007–1011
- Maeda, S., Matsuoka, M., Nakata, N., Kai, M., Maeda, Y., Hashimoto, K., Kimura, H., Kobayashi, K., and Kashiwabara, Y. (2001) Multidrug resistant *Mycobacterium leprae* from patients with leprosy. *Antimicrob. Agents Chemother.* **45**, 3635–3639
- Raku, T., Kitagawa, M., Shimakawa, H., and Tokiwa, Y. (2003) Enzymatic synthesis of trehalose esters having lipophilicity. *J. Biotechnol.* **100**, 203–208
- Kremer, L., Maughan, W.N., Wilson, R.A., Dover, L.G., and Besra, G.S. (2002) The *M. tuberculosis* antigen 85 complex and mycolyltransferase activity. *Lett. Appl. Microbiol.* **34**, 233–237
- Matsunaga, I., Komori, T., Ochi, A., Mori, N., and Sugita, M. (2008) Identification of antibody responses to the serotype-nonspecific molecular species of glycopeptidolipids in *Mycobacterium avium* infection. *Biochem. Biophys. Res. Commun.* **377**, 165–169
- Ogata, K. and Umeyama, H. (2000) An automatic homology modeling method consisting of database searches and simulated annealing. *J. Mol. Graph. Model* **18**, 258–272
- Wheelock, C.E., Nakagawa, Y., Harada, T., Oikawa, N., Akamatsu, M., Smaghe, G., Stefanou, D., Iatrou, K., and Swamers, L. (2006) High-throughput screening of ecdysone agonists using a reporter gene assay followed by 3-D QSAR analysis of the molting hormonal activity. *Bioorg. Med. Chem.* **14**, 1143–1159
- Anderson, D.H., Harth, G., Horwitz, M.A., and Eisenberg, D. (2001) An interfacial mechanism and a class of inhibitors inferred from two crystal structures of the *Mycobacterium tuberculosis* 30 kDa major secretory protein (Antigen 85B), a mycolyl transferase. *J. Mol. Biol.* **307**, 671–681
- Ronning, D.R., Klabunde, T., Besra, G.S., Vissa, V.D., Belisle, J.T., and Sacchetti, J.C. (2000) Crystal structure of the secreted form of antigen 85C reveals potential targets for mycobacterial drugs and vaccines. *Nat. Struct. Biol.* **7**, 141–146
- Ronning, D.R., Vissa, V., Besra, G.S., Belisle, J.T., and Sacchetti, J.C. (2004) *Mycobacterium tuberculosis* antigen 85A and 85C structures confirm binding orientation and conserved substrate specificity. *J. Biol. Chem.* **279**, 36771–36777
- Moody, D.B., Reinhold, B.B., Guy, M.R., Beckman, E.M., Frederique, D.E., Furlong, S.T., Ye, S., Reinhold, V.N., Sieling, P.A., Modlin, R.L., Besra, G.S., and Porcelli, S.A. (1997) Structural requirements for glycolipid antigen recognition by CD1b-restricted T cells. *Science* **278**, 283–286
- Stenger, S., Mazzaccaro, R.J., Uyemura, K., Cho, S., Barnes, P.F., Rosat, J.P., Sette, A., Brenner, M.B., Porcelli, S.A., Bloom, B.R., and Modlin, R.L. (1997) Differential effects of cytolytic T cell subsets on intracellular infection. *Science* **276**, 1684–1687
- Williams, D.L., Torrero, M., Wheeler, P.R., Trunan, R.W., Yoder, M., Morrison, N., Bishai, W.R., and Gillis, T.P. (2004) Biological implications of *Mycobacterium leprae* gene expression during infection. *J. Mol. Microbiol. Biotechnol.* **8**, 58–72



## Etanercept treatment reduces the serum levels of interleukin-15 and interferon-gamma inducible protein-10 in patients with rheumatoid arthritis

Tetsuya Ichikawa · Yasunori Kageyama ·  
Hayato Kobayashi · Norihiko Kato ·  
Kunio Tsujimura · Yukio Koide

Received: 11 November 2009 / Accepted: 29 December 2009  
© Springer-Verlag 2010

**Abstract** Tumor necrosis factor- $\alpha$  (TNF- $\alpha$ ) has an essential role in the pathogenesis of rheumatoid arthritis (RA) and has been known to induce the production of several inflammatory molecules *in vivo*. To analyze *in vivo* the active mechanism of the TNF- $\alpha$  blocking agent, etanercept, the serum levels of the cytokine interleukin-15 (IL-15) and the chemokines growth-regulated protein- $\alpha$  (Gro- $\alpha$ ), and interferon- $\gamma$  inducible protein-10 (IP-10) in RA patients were measured. Twenty-two patients with RA were administered etanercept once or twice a week for more than 6 months. The clinical and laboratory parameters were measured and serum levels of IL-15, Gro- $\alpha$ , and IP-10 were determined using enzyme-linked immunosorbent assay (ELISA) kits at the baseline and at 3 and 6 months after the initial treatment. Additionally, the production of IL-15 and IP-10 by cultured synovial cells stimulated with TNF- $\alpha$  from RA patients was determined by ELISA. A significant decrease in serum levels of IL-15 and IP-10 was observed at 3 and 6 months after initial treatment with etanercept, but not in those of Gro- $\alpha$ . TNF- $\alpha$  induced production of IP-10, but not IL-15 in cultured synovial cells from RA patients. This study demonstrated for the first time the reduction of

IP-10 and IL-15 production in RA patients as active mechanisms of etanercept.

**Keywords** Rheumatoid arthritis · Etanercept · Interleukin-15 · Interferon-gamma inducible protein-10 · Growth-regulated protein-alpha

### Introduction

Tumor necrosis factor- $\alpha$  (TNF- $\alpha$ ) has been considered to be an essential cytokine forming the pathological focus of rheumatoid arthritis (RA) [1, 2] by producing various types of chemokines, cytokines, and reactive oxygen species [3, 4]. Recently, the clinical use of a TNF- $\alpha$  blocking agent for RA patients has brought innovative results including regulation of joint destruction. However, the biological mechanism of TNF- $\alpha$  blocking agents *in vivo* has not been always understood clearly. As one mechanism of the action of TNF- $\alpha$  blocking agents, it has been hypothesized that the levels of several inflammatory chemokines and cytokines decrease. We have previously demonstrated that infliximab reduced the serum levels of interleukin-15 (IL-15) and growth-regulated protein- $\alpha$  (Gro- $\alpha$ ) but not those of interferon- $\gamma$  inducible protein-10 (IP-10) in RA patients [5–7].


IP-10 has various activities including stimulation of the migration of monocytes, natural killer cells and T cells [8] and has been reported to exist at higher levels in the serum and synovial fluid of RA patients [7, 9]. In addition, IP-10 is induced by a variety of inflammatory mediators including TNF- $\alpha$ , interleukin-1 (IL-1), and interferon- $\gamma$  (IFN- $\gamma$ ) [10–12]. IL-15 has been reported to induce the differentiation of osteoclast progenitors into preosteoclasts [13]. Gro- $\alpha$  is detected in the synovial membrane in RA and is a chemokine induced by TNF- $\alpha$  [14, 15].

T. Ichikawa  
Department of Orthopaedic Surgery, Narita Memorial Hospital,  
78 Shirakawa-cho, Toyohashi 441-8021, Japan

Y. Kageyama (✉) · H. Kobayashi · N. Kato  
Department of Orthopaedic Surgery, Heisei Memorial Hospital,  
123-1 Mizugami, Fujieda 426-8662, Japan  
e-mail: Tsukatonpipi@nifty.com

K. Tsujimura · Y. Koide  
Division of Host Defense, Department of Infectious Disease,  
Hamamatsu University School of Medicine,  
1-20-1 Handayama, Higashiku,  
Hamamatsu 431-3192, Japan

Published online: 10 January 2010

 Springer

Etanercept and infliximab both block TNF- $\alpha$ , but do not always show the same effects in clinical use for RA patients. Here, we measured the serum levels of IL-15, Gro- $\alpha$ , and IP-10 before and after treatment by etanercept in RA patients and analyzed the *in vivo* mechanism of etanercept.

## Materials and methods

### RA patients receiving etanercept treatment

Informed consent was obtained from all study participants. Twenty-two patients (20 females and 2 males; mean age  $61.8 \pm 9.1$  years; mean disease duration  $15.3 \pm 7.4$  years; Steinblocker's stage II: 4, III: 14, IV: 4) with RA, diagnosed according to the criteria of the American College of Rheumatology, were evaluated in this study between October 2005 and December 2006. We evaluated the patients administered etanercept for more than 6 months. Thirteen patients received a constant dose of prednisolone (mean dose  $2.4 \pm 2.2$  mg/day) throughout the present study. Etanercept was administered by subcutaneous injection at a dosage of 25 mg once or twice a week. Sixteen patients received etanercept in combination with methotrexate (MTX) perorally at a constant dosage of 4–10 mg/week. Six patients were treated with etanercept alone. The patients treated with etanercept were divided into MTX-treated [MTX (+)] and MTX-nontreated [MTX (-)] groups, and their data were evaluated in total and respective groups.

### Clinical and laboratory evaluation

Clinical and laboratory examinations including erythrocyte sedimentation rate (ESR), C-reactive protein (CRP), anti-galactosyl IgG antibody (CA-RF), and a Disease Activity Score of 28 joints (DAS28) were performed at the baseline and at 3 and 6 months after the initial treatment. Serum samples of RA patients were obtained just before an initial injection of etanercept at the baseline and at 3 and 6 months after the initial treatment with etanercept. The serum levels of IL-15, IP-10, and Gro- $\alpha$  were measured in all patients as described below.

### Measurements of serum levels of IL-15, IP-10, and Gro- $\alpha$

The serum levels of IL-15, IP-10, and Gro- $\alpha$ , and CA-RF from RA patients with etanercept treatment were measured using an enzyme-linked immunosorbent assay (ELISA), following the manufacturer's instructions (IL-15 and IP-10, ELISA kits, Biosource, Nivelles, Belgium; Gro- $\alpha$  ELISA kit, R&D, MN, USA; and CA-RF ELISA kit, Ei Test, Eisai, Tokyo, Japan). All samples were measured in duplicate. To

demonstrate that this assay is not sensitive to rheumatoid factors (RF) interaction, IL-15, IP-10, and Gro- $\alpha$  levels of the serum from five RA patients without infliximab treatment with RF (+) were measured with or without absorption of RF by human IgG (1 mg/ml, 24 h incubation) bound protein G beads, as following our methods described previously [5]. Absorption of RF was made as follows: 100  $\mu$ l of human IgG (1 mg/ml) was mixed with 100  $\mu$ l of protein G beads overnight at room temperature. The beads were washed twice with PBS. The serum samples were incubated with the immunoglobulin-coupled beads (1:1 vols.) for 2 h to eliminate RF. The IL-15, IP-10, and Gro- $\alpha$  levels of the samples, which were incubated with or without immunoglobulin-coupled beads, were assayed. There was no significant difference in these cytokine levels between the no treated serum and the serum incubated with the immunoglobulin-coupled beads (data not shown).

Measurements of the levels of IL-15 and IP-10 produced by cultured synovial cells stimulated with TNF- $\alpha$  or IFN- $\gamma$

Synovial membranes were obtained from 5 patients with RA at total knee arthroplasty. The membranes were finely minced and then digested for 2 h at 37°C with 1 mg/ml of collagenase type I (Sigma, St. Louis, MO, USA). The cells were washed with phosphate-buffered saline and suspended in culture dishes with a 12-cm diameter containing DMEM with 10% fetal bovine serum for 2 weeks and then resuspended at  $1 \times 10^5$  cells/well in culture dishes with a 3.5-cm diameter. The adherent cells in the dish were incubated for 48 h after the addition of IFN- $\gamma$  (50 ng/ml) or TNF- $\alpha$  (0, 10, or 50 ng/ml) (R&D, Minneapolis, MN, USA). The cell-free supernatants were collected and used for IL-15 or IP-10 assays.

### Statistical analysis

All data were shown as the mean  $\pm$  SD. The values in pre- and post-treatment measurements were compared using the Wilcoxon signed rank test. Single regression analysis was performed, and the statistical significance of correlation was determined with Pearson's correlation test. *P* values less than 0.05 were considered to be significant in this study. All statistical analysis was performed on a Macintosh computer using the Statcel software package.

## Results

### Clinical and laboratory disease activity

CRP levels in total RA patients significantly decreased from  $2.02 \pm 0.96$  mg/dl at pretreatment to  $0.63 \pm 0.85$  mg/dl

**Table 1** The serum levels of interleukin-15 (IL-15), interferon- $\gamma$  inducible protein-10 (IP-10), and growth-regulated protein- $\alpha$  (Gro- $\alpha$ ) in patients with RA treated with etanercept was measured at baseline, 3 months, and 6 months after initial treatment with etanercept

	Baseline	3 months	6 months
<b>Serum IL-15 (pg/ml)</b>			
Total	1,117 $\pm$ 784	654 $\pm$ 544**	555 $\pm$ 460***
MTX (+)	1,202 $\pm$ 899	617 $\pm$ 519**	476 $\pm$ 356**
MTX (-)	917 $\pm$ 393	740 $\pm$ 623*	683 $\pm$ 554*
<b>Serum IP-10 (pg/ml)</b>			
Total	395 $\pm$ 291	153 $\pm$ 213**	121 $\pm$ 163**
MTX (+)	430 $\pm$ 334	116 $\pm$ 164**	122 $\pm$ 180**
MTX (-)	300 $\pm$ 81	274 $\pm$ 271	120 $\pm$ 116*
<b>Serum Gro-<math>\alpha</math> (pg/ml)</b>			
Total	219 $\pm$ 340	203 $\pm$ 358	247 $\pm$ 448
MTX (+)	267 $\pm$ 400	244 $\pm$ 426	298 $\pm$ 529
MTX (-)	107 $\pm$ 59	107 $\pm$ 27	120 $\pm$ 23
<b>CRP (mg/dl)</b>			
Total	2.02 $\pm$ 0.96	0.63 $\pm$ 0.85**	0.70 $\pm$ 1.05**
MTX (+)	1.68 $\pm$ 0.72	0.32 $\pm$ 0.22**	0.38 $\pm$ 0.41**
MTX (-)	2.82 $\pm$ 0.99	1.35 $\pm$ 1.30*	1.46 $\pm$ 1.66*
<b>ESR (mm/h)</b>			
Total	55 $\pm$ 17	37 $\pm$ 24**	33 $\pm$ 19**
MTX (+)	59 $\pm$ 18	36 $\pm$ 28**	36 $\pm$ 22**
MTX (-)	48 $\pm$ 11	38 $\pm$ 12*	25 $\pm$ 5.8*
<b>Number of swollen joints</b>			
Total	8.0 $\pm$ 4.0	3.8 $\pm$ 3.2**	3.1 $\pm$ 2.1**
MTX (+)	9.1 $\pm$ 3.7	5.1 $\pm$ 2.9**	4.0 $\pm$ 1.8**
MTX (-)	5.0 $\pm$ 3.4	0.9 $\pm$ 1.1*	1.0 $\pm$ 0.8*
<b>Number of tender joints</b>			
Total	2.5 $\pm$ 1.1	0.3 $\pm$ 0.7**	0.5 $\pm$ 1.2**
MTX (+)	2.6 $\pm$ 1.1	0.4 $\pm$ 0.8**	0.1 $\pm$ 0.4**
MTX (-)	2.6 $\pm$ 1.0	0.6 $\pm$ 1.0	0.3 $\pm$ 0.5*
<b>DAS28-CRP</b>			
Total	4.47 $\pm$ 0.50	2.70 $\pm$ 0.59***	2.20 $\pm$ 0.51***
MTX (+)	4.48 $\pm$ 0.55	2.71 $\pm$ 0.69***	2.81 $\pm$ 0.66***
MTX (-)	4.42 $\pm$ 0.38	2.60 $\pm$ 0.83*	2.94 $\pm$ 0.52*
<b>Serum CA-RF (AU/ml)</b>			
Total	383 $\pm$ 642	469 $\pm$ 898	476 $\pm$ 800
MTX (+)	180 $\pm$ 133	153 $\pm$ 107	217 $\pm$ 199
MTX (-)	788 $\pm$ 993	1,101 $\pm$ 1,354	904 $\pm$ 1,055

The clinical and laboratory data were also obtained at the same time. Data are shown by mean  $\pm$  SD values. Data at 3 and 6 months were compared with those at baseline using Wilcoxon signed rank test. Patients treated with etanercept were divided into methotrexate (MTX) (+) and MTX (-) groups

\*\*  $P < 0.01$  versus baseline, \*  $P < 0.05$  versus baseline

( $P < 0.01$ ) and  $0.70 \pm 1.05$  mg/dl ( $P < 0.01$ ) at 3 and 6 months after the initial injection of etanercept, respectively (Table 1). Those in MTX (+) and MTX (-) patients

receiving etanercept treatment significantly decreased at 3 and 6 months after the initial injection of etanercept, respectively. ESR levels, DAS28-CRP, and number of swelling joints except for serum CA-RF levels were also significantly decreased at 3 and 6 months compared with those at pretreatment.

Measurements of serum levels of IL-15, IP-10, and Gro- $\alpha$  by etanercept treatment

To investigate whether these ELISA systems are sensitive to IL-15, IP-10, and Gro- $\alpha$ , we measured the levels of serum or SF from RA patients after the addition of human IgG for absorption of RF. The addition of human IgG (1 mg/ml) and absorption of RF did not make a statistically significant difference in the IL-15, IP-10, and Gro- $\alpha$  levels (data not shown).

The mean serum IL-15 levels in total RA patients receiving etanercept treatment decreased significantly from  $1,117 \pm 784$  pg/ml at pretreatment to  $654 \pm 544$  pg/ml ( $P < 0.01$ ) and  $555 \pm 460$  pg/ml ( $P < 0.001$ ) at 3 and 6 months after the initial injection of etanercept, respectively (Table 1). Those in MTX (+) and MTX (-) patients receiving etanercept treatment significantly decreased at 3 and 6 months after the initial injection of etanercept, respectively. The mean serum level of IP-10 at pretreatment ( $395 \pm 291$  pg/ml) also decreased significantly at 3 ( $153 \pm 213$  pg/ml) ( $P < 0.05$ ) and 6 months ( $121 \pm 163$  pg/ml) ( $P < 0.01$ ) after the initial injection of etanercept, respectively. Those in MTX (+) patients receiving etanercept treatment significantly decreased at 3 and 6 months after the initial injection of etanercept, respectively. The mean serum IP-10 levels in MTX (-) patients significantly decreased at 6 months. The mean serum Gro- $\alpha$  levels in total, MTX (+), and MTX (-) patients did not show significant differences at 3 and 6 months after the initial injection of etanercept compared with the basic levels.

Correlation analysis among serum IL-15, Gro- $\alpha$ , and IP-10 and other clinical and laboratory parameters

Serum IL-15 levels showed significant correlation with the numbers of tender joints ( $r = 0.470$ ,  $P < 0.05$ ) (Table 2). Serum IP-10 levels significantly correlated with DAS28-CRP levels ( $r = 0.415$ ,  $P < 0.05$ ).

The levels of IL-15 and IP-10 produced by cultured synovial cells stimulated with TNF- $\alpha$  or IFN- $\gamma$

Cultured synovial cells from RA patients were stimulated with TNF- $\alpha$  and IFN- $\gamma$ . TNF- $\alpha$  at the concentrations of 10 and 50 ng/ml significantly induced a large amount of IP-10 production but did not induce a significant change in the

**Table 2** Analysis of correlations between serum IL-15, Gro- $\alpha$ , and IP-10 and other clinical and laboratory parameters in RA patients who received etanercept treatment

	IL-15		Gro- $\alpha$		IP-10	
	Correlation coefficient	<i>P</i> value	Correlation coefficient	<i>P</i> value	Correlation coefficient	<i>P</i> value
CRP	0.275	0.244	-0.199	0.379	0.465	0.244
ESR (1 h)	0.265	0.264	-0.003	0.991	0.160	0.471
CA-RF	0.358	0.122	-0.265	0.278	0.260	0.273
DAS28-CRP	0.389	0.090	-0.366	0.094	0.415*	0.048
Swollen joints	0.154	0.521	-0.348	0.135	0.210	0.340
Tender joints	0.470*	0.035	-0.220	0.331	0.213	0.334

Single regression analysis between serum IL-15, Gro- $\alpha$ , and IP-10 and other clinical and laboratory parameters was performed. The data of sample levels and clinical parameters used in correlation analysis were obtained at the baseline and at 3 and 6 months after initial treatment with etanercept, and data are shown by correlation coefficient. The statistical significance of correlation was determined using Pearson's correlation test

\* *P* < 0.05

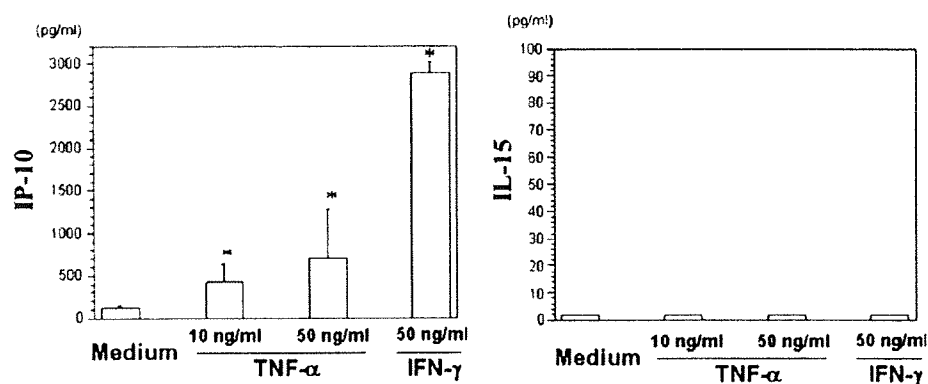


**Fig. 1** The levels of IP-10 and IL-15 produced by cultured synovial cells stimulated with IFN- $\gamma$  or TNF- $\alpha$ . Synovial membranes obtained from RA patients were finely minced and digested for 2 h at 37°C with 1 mg/ml of collagenase type I. The cells were suspended in culture dishes with a 12-cm diameter containing DMEM with 10% fetal bo-

vine serum for 2 weeks and then resuspended at  $1 \times 10^5$  cells/well in culture dishes with a 3.5-cm diameter. The adherent cells in the dish were incubated for 48 h after the addition of IFN- $\gamma$  (50 ng/ml) or TNF- $\alpha$  (0, 10, or 50 ng/ml). The supernatants were collected and the levels of IP-10 and IL-15 were measured by ELISA kits

production of IL-15 (Fig. 1). IFN- $\gamma$  at the concentrations of 50 ng/ml significantly induced a large amount of IP-10 production but did not induce a significant change in the production of IL-15.

## Discussion

TNF- $\alpha$  blocking agents have been shown to affect the production of a variety of cytokines, chemokines, mitogens, and proteases, which may exist at sites downstream of the TNF- $\alpha$  cascade in RA patients [5, 6, 16]. On the other hand, it has been known that TNF- $\alpha$  induces the production of various cytokines and chemokines [6, 17–20]. For instance, there are some reports that IL-15, IP-10, and Gro- $\alpha$  are produced by TNF- $\alpha$  stimulation [21, 22]. Previously we demonstrated that treatment of RA patients with infliximab

decreased their serum levels of IL-15 and Gro- $\alpha$  but did not significantly change those of IP-10 [6, 7]. In the present study, we investigated the effect of etanercept on these proteins. The serum levels of IL-15 and IP-10 in RA patients after etanercept treatment were decreased.

IL-15 stimulates the differentiation of osteoclast progenitors into preosteoclasts [13] and acts at the early stage of osteoclastogenesis. IL-15 has been shown to be responsible for local T cell activation and to stimulate the proliferation of T cells prepared from peripheral blood and synovial fluid samples from RA patients [23]. The synovial fluid of patients with RA was shown to have elevated levels of IL-15 [24], and IL-15 was detected on synovial fibroblasts of RA [23]. In a collagen-induced (CIA) arthritis model known to be an animal model for RA, the soluble IL-15 receptor alpha-chain suppressed the development of CIA [25]. Antagonistic IL-15 mutant/Fc $\gamma$ 2a fusion protein,

which targets the IL-15 receptors, also blocked disease progression in a CIA model [26]. Thus, IL-15 may play a crucial role in the pathogenesis of RA including osteoclastogenesis, which is a cause behind the joint destruction of RA [13]. The decrease of IL-15 production in RA patients after etanercept treatment may elucidate its ability to moderate joint destruction and the existence of the cytokine cascade by which IL-15 is induced by TNF- $\alpha$  in RA patients in vivo. But in our present study, TNF- $\alpha$  stimulation for cultured synovial cells from RA patients did not induce IL-15 production. Ernestam et al. previously reported that the levels of IL-15 in synovial membranes were not significantly unchanged after treatment with infliximab [27]. Taken together, these findings suggest that the production of IL-15 may be indirectly induced by the stimulation of another molecule induced by TNF- $\alpha$ .

IP-10 has been known to be induced by various inflammatory mediators including IL-1, TNF- $\alpha$ , IFN- $\alpha$ , and IFN- $\gamma$ , in monocytes, neutrophils, keratinocytes, fibroblasts, endothelial cells and synovial cells [28–34]. TNF- $\alpha$  enhances phenotypic and functional maturation of human epidermal Langerhans cells and induces IP-10 production [10]. IP-10 has various biological activities, including stimulation of monocyte, natural killer cell and T cell migration, bone marrow progenitor maturation, modulation of adhesion molecule expression, and inhibition of angiogenesis [35]. Furthermore, it was recently reported that IP-10 stimulated the expression of RANKL and TNF- $\alpha$  in CD4+ T cells and showed osteoclastogenic potential in co-cultures of CD4+ T cells and osteoclast precursors [36]. In a CIA model, the levels of RANKL and TNF- $\alpha$  were decreased by an antibody to IP-10, and IP-10 has been shown to be involved in bone erosion in inflamed joints [36]. Indeed, RA synovial fluid (SF) contained greater amounts of IP-10 compared with osteoarthritis SF [37]. IP-10 has been detected on infiltrating macrophage-like cells, and fibroblast-like cells in the RA synovium [38]. Thus, IP-10 is considered to have a relationship with bone destruction that is essential for the pathogenesis of RA. Our data indicated that TNF- $\alpha$  induced the production of IP-10 in the RA synovial membrane in vivo and that etanercept reduced the serum levels of IP-10 in RA patients; therefore, the cascade by which IP-10 is induced by TNF- $\alpha$  stimulation may exist in vivo. The discovery of the reduction of serum levels of IP-10 in RA patients by etanercept treatment is new to this report.

Gro- $\alpha$  levels were not significantly changed after etanercept treatment. However, in our previous study, serum Gro- $\alpha$  levels were significantly decreased after infliximab treatment. Although there is a report that the synovial fluid levels of Gro- $\alpha$  are high in RA patients, the function of Gro- $\alpha$  in the pathogenesis of RA is not yet understood.

Previously, treatment of RA patients with infliximab did not result in a significant change of serum IP-10 levels but decreased the serum Gro- $\alpha$  levels [6, 7]. Although both of etanercept and infliximab are TNF- $\alpha$  blocking agents, they do not always show identical effects in clinical use, even on the same RA patient. This may result from a different mechanism in TNF- $\alpha$  blocking. For example, infliximab has a reverse signal through transmembrane TNF- $\alpha$  on the cell surface [39, 40]. CA-RF levels in RA patients were decreased significantly by infliximab in our previous study, but not by etanercept in the present study [7]. Although the in vivo mechanism of the TNF- $\alpha$  blocker etanercept is not completely understood, the present study provides an important clue. In the present study, we investigated the change of serum levels of IL-15, IP-10, and Gro- $\alpha$  using etanercept; as an additional study, we need to measure the levels of these proteins in the synovial membrane. This may elucidate further the function of the respective TNF- $\alpha$  blocking agents.

**Acknowledgments** In this study, I appreciate the cooperation of the division of host defense at the department of infectious disease in Hamamatsu University School of Medicine for the measurement of the levels of a cytokine and chemokines.

## References

1. Arend WP, Dayer J-M (1995) Inhibition of the production and effects of interleukin-1 and tumor necrosis factor alpha in rheumatoid arthritis. *Arthritis Rheum* 38:151–160
2. Maini RN, Taylor PC (2000) Anti-cytokine therapy for rheumatoid arthritis. *Ann Rev Med* 51:207–229
3. Woo CH, Kim TH, Choi JA, Ryu HC, Lee JE, You HJ et al (2006) Inhibition of receptor internalization attenuates the TNF alpha-induced ROS generation in non-phagocytic cells. *Biochem Biophys Res Commun* 351:972–978
4. Sakon S, Xue X, Takekawa M, Sasazuki T, Okazaki T, Kojima Y et al (2003) NF-kappaB inhibits TNF-induced accumulation of ROS that mediate prolonged MAPK activation and necrotic cell death. *EMBO J* 22:3898–3909
5. Kageyama Y, Takahashi M, Torikai E, Suzuki M, Ichikawa T, Nagafusa T et al (2007) Treatment with anti-TNF-alpha antibody infliximab reduces serum IL-15 levels in patients with rheumatoid arthritis. *Clin Rheumatol* 26:505–509
6. Torikai E, Kageyama Y, Suzuki M, Ichikawa T, Nagano A (2007) The effect of infliximab on chemokines in patients with rheumatoid arthritis. *Clin Rheumatol* 26:1088–1093
7. Kageyama Y, Torikai E, Nagano A (2007) Anti-tumor necrosis factor-alpha antibody treatment reduces serum CXCL16 levels in patients with rheumatoid arthritis. *Rheumatol Int* 27:467–472
8. Neville LF, Mathiak G, Bagasra O (1997) The immunobiology of interferon-gamma inducible protein 10 kD (IP-10): a novel, pleiotropic member of the C-X-C chemokine superfamily. *Cytokine Growth Factor Rev* 8:207–219
9. Hanaoka R, Kasama T, Muramatsu M, Yajima N, Shiozawa F, Miwa Y et al (2003) A novel mechanism for the regulation of IFN-gamma inducible protein-10 expression in rheumatoid arthritis. *Arthritis Res Ther* 5:74–81

10. Berthier-Vergnes O, Bermond F, Flacher V, Massacrier C, Schmitt D, Péguet-Navarro J (2005) TNF-alpha enhances phenotypic and functional maturation of human epidermal Langerhans cells and induces IL-12 p40 and IP-10/CXCL-10 production. *FEBS Lett* 579:60–68
11. Thorburn E, Kolesar L, Brabcova E, Petrickova K, Petricek M, Jaresova M et al (2009) CXC and CC chemokines induced in human renal epithelial cells by inflammatory cytokines. *APMIS* 117:477–487
12. Boorsma DM, de Haan P, Willemze R, Stoof TJ (1994) Human growth factor (huGRO), interleukin-8 (IL-8) and interferon-gamma-inducible protein (gamma-IP-10) gene expression in cultured normal human keratinocytes. *Arch Dermatol Res* 286:471–475
13. Ogata Y, Kukita A, Kukita T, Komine M, Miyahara A, Miyazaki S et al (1999) A novel role of IL-15 in the development of osteoclasts: inability to replace its activity with IL-2. *J Immunol* 162:2754–2760
14. König A, Krenn V, Toksoy A, Gerhard N, Gillitzer R (2000) Mig, GRO alpha and RANTES messenger RNA expression in lining layer, infiltrates and different leucocyte populations of synovial tissue from patients with rheumatoid arthritis, psoriatic arthritis and osteoarthritis. *Virchows Arch* 436:449–458
15. Plater-Zyberk C, Hoogewerf AJ, Proudfoot AE, Power CA, Wells TN (1997) Effect of a CC chemokine receptor antagonist on collagen induced arthritis in DBA/1 mice. *Immunol Lett* 57:117–120
16. Klimiuk PA, Sierakowski S, Domyslawska I, Chwiecko J (2004) Effect of repeated infliximab therapy on serum matrix metalloproteinases and tissue inhibitors of metalloproteinases in patients with rheumatoid arthritis. *J Rheumatol* 31:238–242
17. Zhang HG, Hyde K, Page GP, Brand JP, Zhou J, Yu S et al (2004) Novel tumor necrosis factor alpha-regulated genes in rheumatoid arthritis. *Arthritis Rheum* 50:420–431
18. Zoja C, Wang JM, Bettoni S, Sironi M, Renzi D, Chiaffarino F et al (1991) Interleukin-1 beta and tumor necrosis factor-alpha induce gene expression and production of leukocyte chemotactic factors, colony-stimulating factors, and interleukin-6 in human mesangial cells. *Am J Pathol* 138:991–1003
19. Visser CE, Tekstra J, Brouwer-Steenbergen JJ, Tuk CW, Boorsma DM, Sampat-Sardjoeersad SC et al (1998) Chemokines produced by mesothelial cells: huGRO-alpha, IP-10, MCP-1 and RANTES. *Clin Exp Immunol* 112:270–275
20. Harigai M, Hara M, Yoshimura T, Leonard EJ, Inoue K, Kashiwazaki S (1993) Monocyte chemoattractant protein-1 (MCP-1) in inflammatory joint diseases and its involvement in the cytokine network of rheumatoid synovium. *Clin Immunol Immunopathol* 69:83–91
21. Arend WP, Dayer JM (1990) Cytokines and cytokine inhibitors or antagonists in rheumatoid arthritis. *Arthritis Rheum* 33:305–315
22. Harada S, Yamamura M, Okamoto H, Morita Y, Kawashima M, Aita T, Makino H (1999) Production of interleukin-7 and interleukin-15 by fibroblast-like synoviocytes from patients with rheumatoid arthritis. *Arthritis Rheum* 42:1508–1516
23. Miranda-Carus ME, Balsa A, Benito-Miguel M, Perez de Ayala C, Martin-Mola E (2004) IL-15 and the initiation of cell contact-dependent synovial fibroblast-T lymphocyte cross-talk in rheumatoid arthritis: effect of methotrexate. *J Immunol* 173:1463–1476
24. Raza K, Falciani F, Curnow SJ, Ross EJ, Lee CY, Akbar AN et al (2005) Early rheumatoid arthritis is characterized by a distinct and transient synovial fluid cytokine profile of T cell and stromal cell origin. *Arthritis Res Ther* 7:784–795
25. Ruchatz H, Leung BP, Wei XQ, McInnes IB, Liew FY (1998) Soluble IL-15 receptor alpha-chain administration prevents murine collagen-induced arthritis: a role for IL-15 in development of antigen-induced immunopathology. *J Immunol* 160:5654–5660
26. Ferrari-Lacraz S, Zanelli E, Neuberger M, Donskoy E, Kim YS, Zheng XX et al (2004) Targeting IL-15 receptor-bearing cells with an antagonist mutant IL-15/Fc protein prevents disease development and progression in murine collagen-induced arthritis. *J Immunol* 173:5818–5826
27. Ernestam S, af Klint E, Catrina AI, Sundberg E, Engström M, Klareskog L, Ulfgrén AK (2006) Synovial expression of IL-15 in rheumatoid arthritis is not influenced by blockade of tumour necrosis factor. *Arthritis Res Ther* 8:R18
28. Bédard PA, Golds EE (1993) Cytokine-induced expression of mRNAs for chemotactic factors in human synovial cells and fibroblasts. *Cell Physiol* 154:433–441
29. Boorsma DM, Flier J, Sampat S, Ottevanger C, de Haan P, Hooft L et al (1998) Chemokine IP-10 expression in cultured human keratinocytes. *Arch Dermatol Res* 290:335–341
30. Cassatella MA, Gasperini S, Calzetti F, Bertagnin A, Luster AD, McDonald PP (1997) Regulated production of the interferon-gamma-inducible protein-10 (IP-10) chemokine by human neutrophils. *Eur J Immunol* 27:111–115
31. Ebnet K, Simon MM, Shaw S (1996) Regulation of chemokine gene expression in human endothelial cells by proinflammatory cytokines and *Borrelia burgdorferi*. *Ann N Y Acad Sci* 797:107–117
32. Luster AD, Unkeless JC, Ravetch JV (1985) Gamma-interferon transcriptionally regulates an early-response gene containing homology to platelet proteins. *Nature* 315:672–676
33. Luster AD (1998) Chemokines-chemotactic cytokines that mediate inflammation. *N Engl J Med* 338:436–445
34. Luster AD, Ravetch JV (1987) Biochemical characterization of a gamma interferon-inducible cytokine (IP-10). *J Exp Med* 166:1084–1097
35. Neville LF, Mathiak G, Bagasra O (1997) The immunobiology of interferon-gamma inducible protein 10 kD (IP-10): a novel, pleiotropic member of the C-X-C chemokine superfamily. *Cytokine Growth Factor Rev* 8:207–219
36. Kwak HB, Ha H, Kim HN, Lee JH, Kim HS, Lee S et al (1997) Reciprocal cross-talk between RANKL and interferon-gamma-inducible protein 10 is responsible for bone-erosive experimental arthritis. *Arthritis Rheum* 58:1332–1342
37. Hanaoka R, Kasama T, Muramatsu M, Yajima N, Shiozawa F, Miwa Y et al (2003) A novel mechanism for the regulation of IFN-gamma inducible protein-10 expression in rheumatoid arthritis. *Arthritis Res Ther* 5:74–81
38. Patel DD, Zachariah JP, Whichard LP (2001) CXCR3 and CCR5 ligands in rheumatoid arthritis synovium. *Clin Immunol* 98:39–45
39. Rigby WF (2007) Drug insight: different mechanisms of action of tumor necrosis factor antagonists-passive-aggressive behavior? *Nat Clin Pract Rheumatol* 3:227–233
40. Mitoma H, Horiuchi T, Hatta N, Tsukamoto H, Harashima S, Kikuchi Y et al (2005) Infliximab induces potent anti-inflammatory responses by outside-to-inside signals through transmembrane TNF-alpha. *Gastroenterology* 128:376–392



2<sup>nd</sup> Vaccine Global Congress, Boston 2008

## Induction of anti-tumor immune responses with oligomannose-coated liposomes targeting to peritoneal macrophages

Kunio Tsujimura<sup>a,b,\*</sup>, Yuzuru Ikehara<sup>c,d</sup>, Toshi Nagata<sup>e</sup>, Yukio Koide<sup>f</sup>, Naoya Kojima<sup>g</sup>

<sup>a</sup>Department of Infectious Diseases, Hamamatsu University School of Medicine, 1-20-1 Handa-yama, Higashi-ku, Hamamatsu 431-3192, Japan

<sup>b</sup>Division of Immunology, Aichi Cancer Center Research Institute, 1-1 Kanokoden, Chikusa-ku, Nagoya 464-8681, Japan

<sup>c</sup>Molecular Medicine Team of Research Center for Medical Glycoscience, National Institute of Advanced Industrial Science and Technology, Central 2-12, Room 211, 1-1-1 Umezono, Tsukuba 305-8568, Japan

<sup>d</sup>Division of Oncological Pathology, Aichi Cancer Center Research Institute, 1-1 Kanokoden, Chikusa-ku, Nagoya 464-8681, Japan

<sup>e</sup>Department of Health Science, Hamamatsu University School of Medicine, 1-20-1 Handa-yama, Higashi-ku, Hamamatsu 431-3192, Japan

<sup>f</sup>Director, Hamamatsu University School of Medicine, 1-20-1 Handa-yama, Higashi-ku, Hamamatsu 431-3192, Japan

<sup>g</sup>Department of Applied Biochemistry, The Institute of Glycotechnology, Tokai University, 1117 Kitakaname, Hiratsuka 259-1292, Japan

### Abstract

We recently established a novel drug delivery system (DDS) using oligomannose-coated liposomes (OMLs) taken up by peritoneal phagocytic cells to carry anti-cancer drugs to milky spots known as a preferential metastatic site of gastric cancers (Ikehara *et al.* 2006. *Cancer Res.* 66: 8740-8748). In the present study, we applied this intraperitoneal DDS for systemic tumor immunotherapy employing ovalbumin (OVA) as a model antigen. The phagocytic cells ingesting the OMLs containing OVA (OML-OVA) injected into the peritoneal cavity were predominantly macrophages ( $M\phi$ ), as they showed adhesive characteristics and expressed F4/80 and CD11b almost exclusively. Peritoneal  $M\phi$  taking up OML-OVA could activate OVA-specific CD8<sup>+</sup> (from OT-I: OVA<sub>257-264</sub>/H-2K<sup>b</sup>-specific) and CD4<sup>+</sup> (from OT-II: OVA<sub>323-339</sub>/H-2A<sup>b</sup>-specific) T cells much more effectively *in vitro* than those taking up soluble OVA. Furthermore, only the mice immunized with OML-OVA rejected E.G7-OVA (OVA-transfected EL4) but not EL4. These results indicate that the OMLs can also be used as an effective antigen delivery system for tumor immunotherapy activating both CD8<sup>+</sup> and CD4<sup>+</sup> T cell subsets.

© 2009 Elsevier B.V. All rights reserved

**Key words:** Oligomannose-coated liposome; Antigen delivery system; Tumor immunotherapy; Macrophage

\* Corresponding author. Kunio Tsujimura Tel.: +81-53-435-2335; fax: +81-53-435-2335.  
E-mail address: [ktsujimu@hama-med.ac.jp](mailto:ktsujimu@hama-med.ac.jp)

## 1. Introduction

Recent advances in tumor immunology enable us to identify tumor antigens recognized by T cells and understand the molecular and cellular bases of T cell-mediated anti-tumor responses (1, 2). However, there are several problems left for the establishment of effective immunotherapy against solid tumors. Many CD8<sup>+</sup> and CD4<sup>+</sup> T cells recognizing tumor antigens in the context of MHC class I and II, respectively, have been reported, and the former are known to be a major effector of the adaptive anti-tumor immune responses (3-5). CD4<sup>+</sup> T cells play an important role for the expansion and persistence of CD8<sup>+</sup> T cells, while some of them are known to function as regulatory cells (5-7). Optimal anti-tumor immune responses are therefore considered to require the concomitant activation of both CD8<sup>+</sup> and CD4<sup>+</sup> T cells and the selective activation of CD4<sup>+</sup> T cells with helper but not regulatory functions (8). In general, endogenous and exogenous antigens are presented as peptides preferentially by MHC class I and II, respectively, and most tumor antigen peptides are derived from the proteins expressed endogenously. Novel methods to induce effective antigen presentation by MHC class I and II molecules simultaneously are therefore needed for the concomitant activation of tumor antigen-specific CD8<sup>+</sup> and CD4<sup>+</sup> T cells, and many attempts have been made for this purpose (2, 3, 8).

We recently developed a novel drug delivery system (DDS) using oligomannose-coated liposomes (OMLs) (9, 10) which are effectively taken up by F4/80<sup>+</sup> peritoneal cells to carry anti-cancer drugs to milky spots known as a preferential metastatic site of gastric and ovarian cancers (9). We demonstrated that this system could control the formation of overt metastasis of seeded gastric cancer cells at the extra-nodal lymphoid tissues such as the omentum (10-12).

In the present study, we applied this OML-based intraperitoneal DDS for tumor immunotherapy using ovalbumin (OVA) as a model antigen, aiming at the concomitant activation of antigen-specific CD8<sup>+</sup> and CD4<sup>+</sup> T cells. Peritoneal macrophages (*M*φ) took up OMLs containing OVA (OML-OVA) and activated both OVA-specific CD8<sup>+</sup> and CD4<sup>+</sup> T cells effectively *in vitro*. In addition, OML-OVA immunized mice rejected tumor cells expressing OVA but not their parental cells. These results together indicate the potential of our novel OML-based immunization for the development of effective tumor immunotherapy.

## 2. Materials and methods

**Mice.** Female C57BL/6 (B6) mice at 8-12 weeks of age were obtained Charles River Japan Inc. (Yokohama, Japan). T cell receptor (TCR) transgenic mice OT-I (specific for OVA<sub>257-264</sub> peptide presented by H-2K<sup>b</sup>) (13, 14) and OT-II (specific for OVA<sub>323-339</sub> peptide presented by H-2A<sup>b</sup>) (15) were obtained from the Jackson Laboratory (Bar Harbor, ME). All animal experiments were performed under the experimental protocol approved by the Ethics Review Committee for Animal Experimentation of Aichi Cancer Center.

**Cell lines.** EL4 (16), a B6-derived thymoma cell line, was maintained in RPMI1640 medium (Invitrogen, Carlsbad, CA) supplemented with 8% fetal bovine serum, 0.2% L-glutamine, 100 U/ml penicillin, 100 μg/ml streptomycin, 0.1% HEPES, 0.1 mM non-essential amino acids, 1 mM sodium pyruvate, and 50 μM 2-ME (complete RPMI). E.G7-OVA (EL4 transfected with *OVA* gene) (17) was obtained from ATCC (Manassas, VA) and maintained in complete RPMI supplemented with 400 μg/ml G418 (Wako, Osaka, Japan) in a humidified 5% CO<sub>2</sub> incubator at 37°C.

**Man3-DPPE and liposome preparation.** Dipalmitoylphosphatidylcholine (DPPC), cholesterol, and dipalmitoylphosphatidylethanolamine (DPPE) were purchased from Sigma-Aldrich (St. Louis, MO). Mannotriose (Man3: Manα1-6(Manα1-3)Man) was purchased from Funakoshi (Tokyo, Japan). Man3-DPPE was prepared by conjugation of the mannotriose with DPPE by reductive amination as described previously (10, 18). The purity of Man3-DPPE was confirmed by high-performance thin-layer chromatography (Silica gel 60 HPTLC plate, MERCK, Darmstadt, Germany) and time-of-flight mass spectrometry (Auto FLEX, Bruker Daltonics, Bremen, Germany). The purified Man3-DPPE was quantified by determination of the phosphate contained.

OMLs were prepared as described previously (10). Briefly, a chloroform-methanol (2:1, v/v) solution containing 1.5 μmol of DPPC and 1.5 μmol of cholesterol was placed in a conical flask and dried by rotary evaporation. Subsequently, 2 ml ethanol containing 0.15 μmol of Man3-DPPE was added to the flask and evaporated to prepare a lipid film containing neoglycolipids. Procedures for protein-encasing into OMLs were performed as described



previously (10). The multilamellar vesicles were generated with either 200  $\mu$ l of FITC-labeled or non-labeled OVA (5.0 mg/ml, Sigma-Aldrich) in the dried lipid film by intense vortex dispersion. The multilamellar vesicles were extruded 10 times through polycarbonate membranes of 1  $\mu$ m pore (Nucleopore, Pleasanton, CA). OMLs entrapping proteins were separated from free proteins by four successive rounds of washing in PBS with centrifugation (20,000  $\times$  g, 30 min) at 4°C. The amounts of entrapped proteins were measured using a modified Lowry protein assay reagent (Pierce Biotechnology, Inc., Rockford, IL) in the presence of 0.3% (w/v) sodium dodecyl sulfate using bovine serum albumin as a standard.

**Flow cytometry.** One hour after intraperitoneal injection of OMLs containing FITC-OVA, peritoneal cells were recovered from B6 mice with 5 ml ice cold PBS. Peritoneal cells were incubated on ice for 30 min with PE-labeled antibodies after blocking with mouse Fc Blocker (BD Biosciences, San Jose, CA) and then analysed on a FACSCalibur (BD Biosciences). The following monoclonal antibodies used in this study were purchased or kindly provided: anti-F4/80 (A3-1, Serotec Ltd., Oxford, UK), anti-MHC class II (M5/114.15.2, e-Bioscience, Boston, MA), anti-CD11b (M1/70.15, Caltag Laboratories, Burlingame, CA), anti-CD3 $\epsilon$  (145-2C11, BD Biosciences), anti-CD19 (1D3, BD Biosciences), and anti-H-2K<sup>b</sup>D<sup>b</sup> (20-8-4S, Dr. E. Nakayama, Okayama University).

**In vitro activation of OVA-specific T cells.** One hour after injection of either OML-OVA or soluble OVA into the peritoneal cavity of B6 mice, peritoneal cells were recovered with 5 ml ice cold PBS. The suspended peritoneal cells in complete RPMI were seeded into a 96-well culture plate (5  $\times$  10<sup>5</sup> cells in each well) and incubated overnight at 37°C in a humidified 5% CO<sub>2</sub> incubator. On the next day, non-adherent cells were washed out with complete RPMI, and the adherent cells preferentially consisting of M $\phi$  were co-cultured with 5  $\times$  10<sup>5</sup> cells of either CD8<sup>+</sup> or CD4<sup>+</sup> T cells from the spleen of OT-I and OT-II mice, respectively. CD8<sup>+</sup> and CD4<sup>+</sup> T cells were prepared with the isolation kits for corresponding subsets (Miltenyi Biotec GmbH, Bergisch Gladbach, Germany). The supernatants were collected at 24 h and assayed for IFN- $\gamma$  production with Mouse IFN- $\gamma$  ELISA kit (Pierce).

**In vivo tumor growth.** B6 mice were immunized three times biweekly by peritoneal injection of 1  $\mu$ g OML-OVA. One week after the final immunization, tumor cells were injected subcutaneously into the backs of mice, and the survival time was observed.

### 3. Results

**OMLs are taken up preferentially by peritoneal M $\phi$**  We showed that OMLs are incorporated very effectively by peritoneal cells expressing F4/80 and that the OML-ingesting cells are very useful drug delivery vehicles for tumor chemotherapy (9, 10). To verify whether the OMLs are applicable also for tumor immunotherapy, we first analyzed the F4/80<sup>+</sup> peritoneal cells in detail. FITC-labeled OVA was encased in OML and injected into the peritoneal cavity of B6 mice. One hour after the OML injection, peritoneal cells were collected and analyzed. As shown in Figure 1, peritoneal cells were divided into three groups based on the incorporation of OMLs. Most OVA<sup>high</sup> cells expressed F4/80 and CD11b but not CD3 and CD19, and this population could be removed by plastic adherence. These observations together suggest that OVA<sup>high</sup> population preferentially consists of M $\phi$ . The peritoneal cells with lower OML uptake (OVA<sup>low</sup>) did not express F4/80, and nearly 2/3 of them were considered to be B cells because of their CD19 expression.

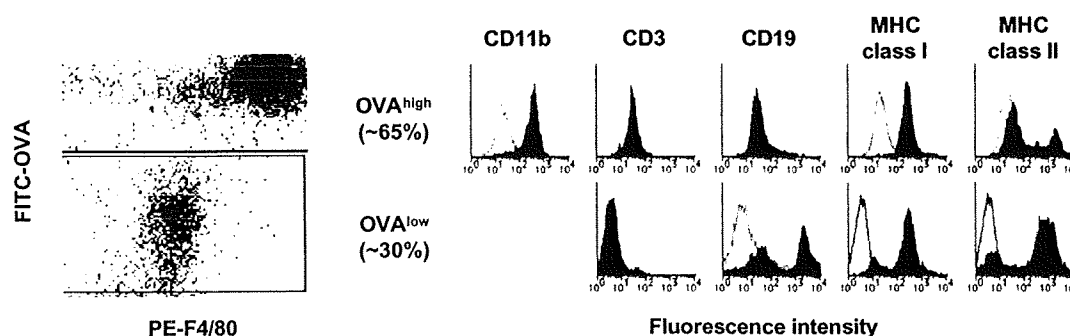


Figure 1. Surface phenotype of peritoneal cells from OML-injected mice. One hour after the injection of OMLs containing FITC-labeled OVA, peritoneal cells were collected and their surface phenotype was analyzed by flow cytometry.

**Peritoneal M $\phi$  ingesting OML-OVA activate both CD8<sup>+</sup> and CD4<sup>+</sup> T cells in vitro in an antigen-specific manner.** We next analyzed the antigen-presenting capacity of the peritoneal M $\phi$  ingesting OML-OVA. CD8<sup>+</sup> T cells from OT-I (OVA<sub>257-264</sub>/H-2K<sup>b</sup>-specific) and CD4<sup>+</sup> T cells from OT-II (OVA<sub>323-339</sub>/H-2A<sup>b</sup>-specific) were used as responder cells. When these T cells were co-cultured with peritoneal M $\phi$  from the mice intraperitoneally injected with OML-OVA, both CD8<sup>+</sup> and CD4<sup>+</sup> T cells produced large amounts of IFN- $\gamma$  (Figure 2). Although M $\phi$  from the mice injected with soluble OVA also stimulated both CD8<sup>+</sup> and CD4<sup>+</sup> T cells, much higher amounts of OVA were needed compared to those from the mice injected with OML-OVA. We also found that cytotoxic T lymphocytes (CTL) against E.G7-OVA can be effectively induced in B6 mice immunized with OML-OVA (data not shown).

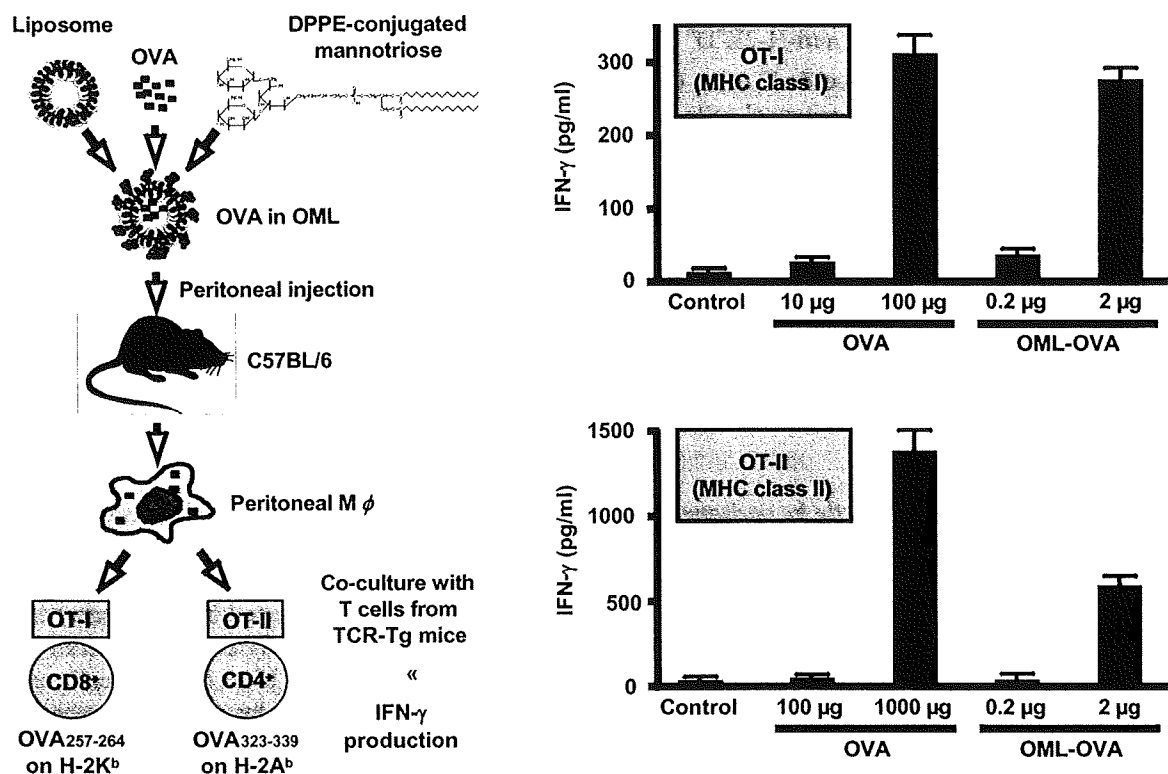


Figure 2. Peritoneal M $\phi$  ingesting OML-OVA activate OVA-specific CD8<sup>+</sup> and CD4<sup>+</sup> T cells much more effectively than those ingesting soluble OVA. One hour after intraperitoneal injection of antigens, peritoneal cells were prepared from the immunized mice, and M $\phi$  were enriched by plastic adherence. CD8<sup>+</sup> and CD4<sup>+</sup> T cells were purified from the spleen of OT-I and OT-II, respectively, and co-cultured with peritoneal M $\phi$  for 24 h. The supernatants were then collected and assayed for IFN- $\gamma$  production by ELISA. Peritoneal M $\phi$  obtained from naïve mice were also used as a control.

**OML-mediated immunization induces antigen-specific anti-tumor immunity in vivo.** We finally examined whether intraperitoneal immunization with OMLs also induces antigen-specific anti-tumor immunity *in vivo*. Mice were immunized intraperitoneally with OML-OVA and then challenged subcutaneously with E.G7-OVA or EL4. As shown in Figure 3, only the immunized mice survived for more than 70 days when challenged with E.G7-OVA, while naïve mice died within 55 days. All the mice including those immunized with OML-OVA died within 30 days when challenged with EL4, indicating that the rejection of E.G7-OVA is OVA-specific. These results

together show that OML-mediated immunization can induce systemic immune response robust enough to protect mice from tumor challenge in an antigen-specific manner.

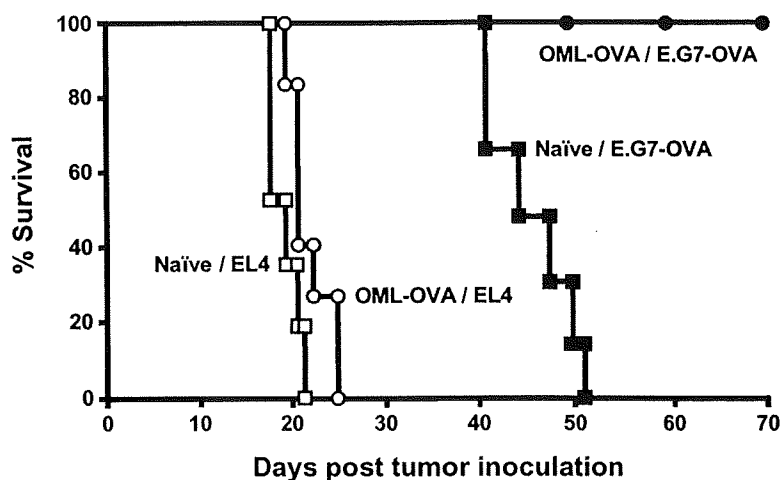


Figure 3. OML-mediated immunization induces antigen-specific anti-tumor immunity *in vivo*. B6 mice were immunized three times biweekly by peritoneal injection of 1  $\mu$ g OML-OVA. One week after the last challenge, OML-OVA immunized (circles) and naïve (squares) mice were challenged subcutaneously with E.G7-OVA (closed symbols) or EL4 (open symbols).

#### 4. Discussion

In this study, we demonstrated that our novel OML-based DDS targeted to peritoneal  $M\phi$  can also be used for the induction of systemic immune responses. After ingesting OML-OVA,  $M\phi$  migrate to extra-nodal lymphoid tissues in abdominal cavity and present OVA-derived peptides in the context of both MHC class I and II molecules. Only the mice immunized with OML-OVA rejected the challenge of E.G7-OVA but not EL4. These results together indicate that the OMLs can be used as an effective antigen delivery system for tumor immunotherapy activating both  $CD8^+$  and  $CD4^+$  T cell subsets as well as a DDS for tumor chemotherapy (Figure 4).

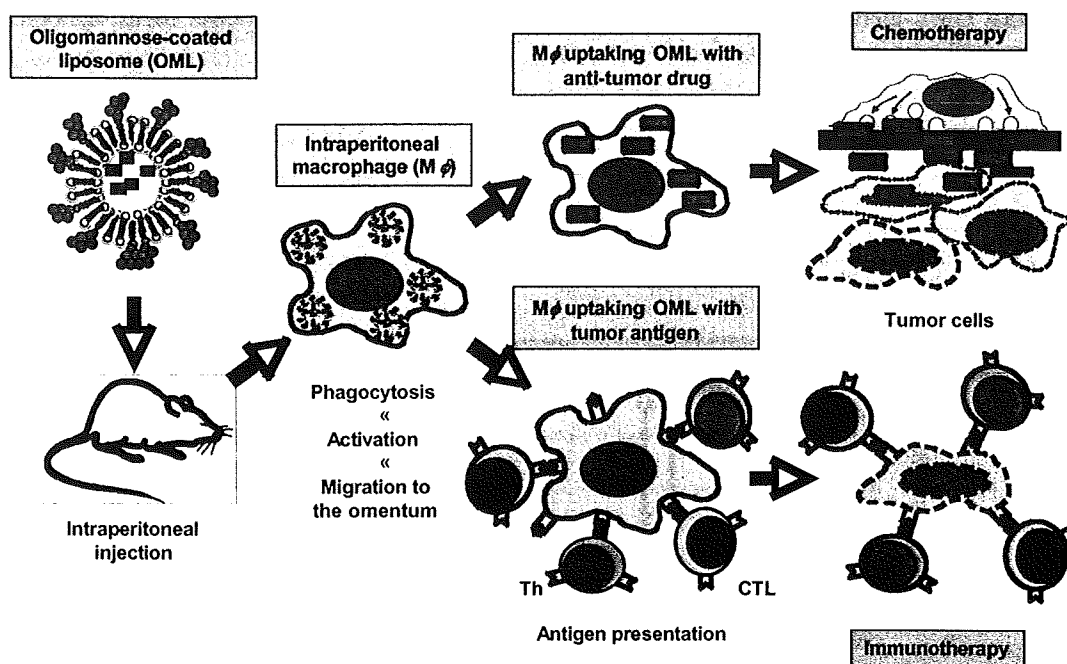


Figure 4. Applications of OMLs for tumor treatment.

OMLs are very useful not only for the promotion of antigen uptake by antigen-presenting cells but also for the enhancement of antigen processing of encased antigens. In general, endogenous and exogenous antigens are presented preferentially by MHC class I and II, respectively. OML-encased antigens, however, were effectively directed to both pathways, even when added exogenously. This advantage of OML-mediated immunization will hopefully facilitate the simultaneous activation of tumor-specific CD4<sup>+</sup> and CD8<sup>+</sup> T cells as shown in this study with OVA. In addition, intraperitoneal uptake of OMLs also induces M $\phi$  maturation with up-regulation of MHC class II and co-stimulatory molecules and IL-12 production, resulting in an effective induction of antigen-specific type 1 helper T cell (Th1) responses (19, 20). Indeed, OT-I and OT-II T cells stimulated with M $\phi$  ingesting OML-OVA produced IFN- $\gamma$  but not IL-4 or IL-10 (Figure 2 and unpublished observation).

Recently, we have shown that OMLs activate phosphatidylinositol 3-kinase/Akt pathway through phosphorylation of Src family kinases to induce the activation of mitogen-activated protein kinases in M $\phi$ -like J774A.1 cells (21). We have also shown that peritoneal M $\phi$  uptake OMLs through a cooperation of specific ICAM-3 garbbling nonintegrin-related 1 (SIGNR1) and complement receptor type 3 (CR3) (22, 23). Thus, SIGNR1 (maybe together with CR3) may associate with nonreceptor-type tyrosine kinases in lipid rafts during OML recognition, and complexes of these molecules facilitate subsequent OML uptake and signal transduction to induce an OML-induced Th1 response.

In order to apply our OMLs in clinical study, the best administration routes should be determined to pursue repetitive vaccination while avoiding possible side effects. As generally acknowledged, intraperitoneal administration is accompanied with a high risk of side effects such as catheter-related complications and abdominal pain. Indeed, it is difficult to complete repetitive intraperitoneal chemotherapy in some cases due to such side effects (24). In this connection, we have already obtained effective *in vivo* anti-tumor responses by subcutaneous injection of OMLs containing tumor antigens (25). However, side effects induced by subcutaneous injection of OMLs should be further investigated to assure their safe clinical application.

In the previous study, we reported that the formation of peritoneal metastasis of seeded gastric cancer cells in milky spots can be controlled with OMLs containing anti-cancer drugs (10). In the present study, we have further extended the possibility of OMLs for the immunotherapy of systemic metastasis and existing tumor cells aside from milky spots. Oligomannose-coating of liposomes showed the best uptake efficiency by peritoneal M $\phi$  among the neoglycolipids so far tested, and the encased antigen was effectively presented by both MHC class I and II